

MULTIPLY ACCELERATED VALUE ITERATION FOR NON-SYMMETRIC AFFINE FIXED POINT PROBLEMS AND APPLICATION TO MARKOV DECISION PROCESSES

MARIANNE AKIAN*, STÉPHANE GAUBERT†, ZHENG QU‡, AND OMAR SAADI†‡

Abstract. We analyze a modified version of Nesterov accelerated gradient algorithm, which applies to affine fixed point problems with non self-adjoint matrices, such as the ones appearing in the theory of Markov decision processes with discounted or mean payoff criteria. We characterize the spectra of matrices for which this algorithm does converge with an accelerated asymptotic rate. We also introduce a d th-order algorithm, and show that it yields a multiply accelerated rate under more demanding conditions on the spectrum. We subsequently apply these methods to develop accelerated schemes for non-linear fixed point problems arising from Markov decision processes. This is illustrated by numerical experiments.

Key words. Nonexpansive maps, dynamic programming, optimal control, large scale optimization, Nesterov acceleration, value iteration, Krasnosel'skiĭ-Mann algorithm, fixed point problems.

1. Introduction. The dynamic programming method reduces optimal control and repeated zero-sum game problems to fixed point problems involving non-linear operators that are order preserving and sup-norm nonexpansive, see [5, 29] for background. The 0-player case, with a finite number n of states, is already of interest. In this case, the involved operator is $T : \mathbb{R}^n \rightarrow \mathbb{R}^n$ of the form $T(x) = g + Px$, where $g = (g_i) \in \mathbb{R}^n$ and $P = (P_{ij}) \in \mathbb{R}^{n \times n}$ is a substochastic matrix, i.e. a matrix with nonnegative entries such that the sum of each row is less than or equal to 1. The scalar g_i is an instantaneous payment received in state i , whereas P_{ij} is the transition probability from i to j . The difference $1 - \sum_j P_{ij}$ is the probability that the process terminates, when in state i . If v is a fixed point of T , the entry v_i yields the expected cost-to-go from the initial state i . More generally, in the one player case (Markov decision processes), one needs to solve a non-linear fixed point problem, described in Section 5, in which the operator T is now a supremum of affine operators $x \mapsto g + Px$.

The standard method to obtain the fixed point of T is to compute the sequence $x_k = T(x_{k-1})$, this is known as *value iteration* [5]. In the 0-player case, value iteration has an asymptotic (geometric) convergence rate given by the spectral radius of P . In many applications, this spectral radius is of the form $1 - \epsilon$ where ϵ is *small*. E.g., ϵ may represent a discount rate. We look for *accelerated* fixed point algorithms, with a convergence rate $1 - \Omega(\epsilon^{1/d})$ for some $d \geq 2$, i.e. a convergence rate that is smaller than $1 - c\epsilon^{1/d}$ for some constant $c > 0$.

In the special case of 0-player problems with a *symmetric* matrix P , an algorithm with a rate $1 - \Omega(\epsilon^{1/2})$ can be obtained by specializing the accelerated gradient algorithm of Nesterov [26]. The latter algorithm applies to the minimization of a smooth strictly convex function f , which, in the quadratic case, reduces to an affine fixed point problem with a symmetric matrix P . See [13]. In contrast, developing accelerated algorithms for problems of non-symmetric type is a challenging question, which has been studied recently in [19, 16].

We study here the affine fixed point problem $x = g + Px$ where the matrix P is non symmetric, and possibly not substochastic. **Theorem 3.3**, one of our main results, states that

*INRIA and CMAP, École polytechnique, IP Paris, CNRS. Address: CMAP, Ecole polytechnique, Route de Saclay, 91128 Palaiseau Cedex, France (emails: marianne.akian@inria.fr, stephane.gaubert@inria.fr, omar.saadi@polytechnique.edu).

†Department of Mathematics, The University of Hong Kong. Address: The University of Hong Kong, Pokfulam Road, Hong Kong (email: zhengqu@hku.hk).

‡O. Saadi acknowledges the support of the Hassan II Academy of Science and Technology. The authors acknowledge the support of the Gaspard Monge (PGMO) program of Fondation Mathématique Hadamard, EDF, Orange and Thales, of the ICODE institute of Paris-Saclay, and of the "Investissement d'avenir" référence ANR-11-LABX-0056-LMH, LabEx LMH. Z. Qu acknowledges the support of Hong Kong Research Grants Council No. 27302016.

a modification of Nesterov’s scheme [26] does converge with an asymptotic rate $1 - \epsilon^{1/2}$ if the spectrum of P is contained in an explicit region of the complex plane, obtained as the image of the disk of radius $1 - \epsilon$ by a rational function of degree 2. We also show that the incorporation of a Krasnosel’skiĭ-Mann type damping [25, 22] (see Equation (2.4a)) enlarges the admissible spectrum region of P for acceleration, see Theorem 3.7. Moreover, we introduce a new scheme (2.8), of order $d \geq 2$, and show in Theorem 4.3 that it leads to a multiply accelerated asymptotic rate of $1 - \epsilon^{1/d}$, but under a more demanding condition on the spectrum of P , see Theorem 4.3. This theorem also shows that this condition is tight. However, slightly more flexible conditions suffice to guarantee a rate of $1 - \Omega(\epsilon^{1/d})$, as shown by Theorem 4.9.

We subsequently apply the proposed schemes and theoretical results, concerning the affine “0-player case”, to solve non-linear fixed point problems arising from Markov decision processes. We use policy iteration, which allows a reduction to a sequence of affine fixed point problems, still benefiting of acceleration for the solution of each affine problem. This leads to an accelerated policy iteration algorithm (see Algorithm 4.1), which produces an approximate solution with a precision of order $((1 + \gamma)\delta + \delta')/(1 - \gamma)^2$ where γ is the maximal discount factor, δ is the accuracy of each inner affine problem and δ' is the accuracy of the policy improvement, see Proposition 4.11.

In Section 5, we show the performance of the simple and multiple acceleration schemes, on classes of instances in which the spectral conditions for acceleration are met. In Subsection 5.1, we consider a framework of random matrices that shows distributions of eigenvalues [9] that are compatible with the spectral conditions required for the convergence of the simple and multiple acceleration schemes proposed here. In Subsection 5.2, we show the performance of the accelerated schemes in solving a Hamilton-Jacobi-Bellman equation in the case of small drifts. This example illustrates the usefulness of Theorem 3.4 that allows to have a more tolerant accelerable region on the complex plane while still benefiting from an accelerated asymptotic rate of $1 - \Omega(\epsilon^{1/2})$.

The recent works [19, 16] also deal with generalizations of Nesterov’s accelerated algorithm to solve fixed point problems. Their theoretical convergence results apply to matrices with a real spectrum, showing that the original choice of parameters for Nesterov’s method in the symmetric case still yields an acceleration in this setting. In contrast, we allow a complex spectrum and characterize the region of the complex plane containing spectra of matrices for which the acceleration is valid (see Theorem 3.3 and Theorem 3.7). Also, a main novelty of the present work is the analysis of multiple accelerations (2.8). The idea of applying Nesterov’s acceleration to Markov decision processes appeared in [16], in which a considerable experimental speedup is reported on random instances. The algorithm there coincides with one of the algorithms studied here – 2-accelerated value iteration for Markov decision processes. It is an open problem to establish the convergence of this method for large enough classes of Markov decision processes. The characterization of the set of “accelerable” 0-player problems that we provide here explains why this problem is inherently difficult: in the 0-player problem, the convergence conditions are governed by fine spectral properties which have no known non-linear analogue in the one-player case.

Apart from being applied to Markov decision processes, fixed point iteration also includes as a special case the proximal point method [32], when the mapping T corresponds to the resolvent of a maximal monotone operator. The proximal point method covers a list of pivotal algorithms in optimization such as the proximal gradient descent, the augmented Lagrangian method (ALM) [31] and the alternating directional method of multipliers (ADMM) [12]. The development of accelerated proximal point method has thus attracted a lot of attention [10, 3, 2] and a recent paper [21] constructed a new algorithm achieving $\|x_k - T(x_k)\| \leq O(1/k)$ through the performance estimation problem (PEP) approach [11].

In a more general setting when T is a nonexpansive mapping in a Euclidean norm, a version of Halpern's iteration was recently shown to yield a residual $\|x_k - T(x_k)\| \leq O(1/k)$ [24], also via the PEP approach. These results improve over the worst case bound $\|x_k - T(x_k)\| \leq O(1/\sqrt{k})$ of the Krasnoselski-Mann's iteration for a nonexpansive mapping (in arbitrary norm) [4]. The acceleration results in the above cited works do not overlap with ours as they only apply to nonexpansive mappings in a Euclidean norm. Moreover, in this paper we consider strictly contractive mapping and thus focus on linear instead of sublinear convergence guarantees.

There is also a large body of literature on (quasi-)Newton type methods for solving non-linear equations [30, 20, 37], which can be naturally employed for solving fixed point problem and yield fast asymptotic convergence rate. It is well-known that such methods converge only when close enough to the solution. Some papers proposed various safe-guard conditions to globalize the convergence [36, 40] and do not provide a rate of convergence. We formally characterize the spectrum condition and the faster convergence rate of accelerated value iteration for affine fixed point problem.

The paper is organized as follows. In [Section 2](#) we introduce the accelerated value iteration (AVI) of any degree $d \geq 2$. In [Section 3](#) we provide a formal analysis of AVI of degree 2. In [Section 4](#) we analyze AVI of arbitrary degree $d \geq 2$ and also present the application to Markov decision processes. In [Section 5](#) we provide numerical experimental results.

2. Accelerated Value Iteration. Nesterov proposed in [26, 27] to accelerate the gradient descent scheme for the minimization of a μ -strongly convex function $f : \mathbb{R}^n \rightarrow \mathbb{R}$ whose gradient is of Lipschitz constant L , by adding an inertial step:

$$(2.1a) \quad x_{k+1} = y_k - h\nabla f(y_k) \quad ,$$

$$(2.1b) \quad y_{k+1} = x_{k+1} + \alpha(x_{k+1} - x_k) \quad ,$$

where $0 < h$, and $\alpha \in [0, 1]$ are parameters. Let x_* be the minimizer of f . When $\alpha = 0$, (2.1) reduces to gradient descent. With the step $h = 1/L$, the gradient descent converges linearly with a rate $1 - 2\mu/(L + \mu)$. Indeed, we have $\|x_k - x_*\|^2 \leq (1 - 2\mu/(L + \mu))^k \|x_0 - x_*\|^2$, and $f(x_k) - f(x_*) \leq \frac{L}{2} (1 - 2\mu/(L + \mu))^k \|x_0 - x_*\|^2$, for all $k \geq 1$, see Theorem 2.1.14 in [27]. Moreover, Theorem 2.2.3, *ibid.*, implies that if we choose

$$(2.2) \quad \alpha = \frac{1 - \sqrt{\mu/L}}{1 + \sqrt{\mu/L}},$$

still with $h = 1/L$, the scheme (2.1) converges linearly with a rate $1 - \sqrt{\mu/L}$. Indeed, with α given by (2.2), we have $f(x_k) - f(x_*) \leq 2(1 - \sqrt{\mu/L})^k (f(x_0) - f(x_*))$ for all $k \geq 1$. Note that when the condition number L/μ is large, i.e. $L/\mu \gg 1$, the rate $1 - \sqrt{\mu/L}$ improves over $1 - 2\mu/(L + \mu)$, whence the scheme (2.2) is commonly known as *accelerated gradient descent*.

We consider the fixed point problem for the operator

$$(2.3) \quad T(x) = g + Px \quad .$$

Here, we allow the vector x and the matrix P to have complex entries, requiring only the spectral radius of the matrix P to be strictly less than 1. In the application to MDPs, the vector x will be real and the matrix P will be nonnegative. By abuse of notation, we denote by x_* the unique fixed point of T . We study the *Accelerated Value Iteration algorithm (AVI)* for computing a fixed point of the operator T . It makes a Krasnosel'skiĭ-Mann (KM) type

damping of parameter $0 < \beta \leq 1$, replacing T by $(1 - \beta)I + \beta T$, followed by a Nesterov acceleration step:

$$(2.4a) \quad x_{k+1} = (1 - \beta)y_k + \beta T(y_k) ,$$

$$(2.4b) \quad y_{k+1} = x_{k+1} + \alpha(x_{k+1} - x_k) .$$

When $\alpha = 0$ and $\beta = 1$, the scheme (2.4) reduces to the standard fixed point iteration algorithm:

$$(2.5) \quad x_{k+1} = g + Px_k .$$

When the spectral radius of P is smaller than $1 - \epsilon$ for some $\epsilon \in (0, 1)$, the standard fixed point scheme converges with an asymptotic rate no greater than $1 - \epsilon$ to the unique fixed point, meaning that for any norm $\|\cdot\|$

$$\limsup_{k \rightarrow \infty} \|x_k - x_*\|^{1/k} \leq 1 - \epsilon .$$

By analogy with accelerated gradient descent, we aim at accelerating the standard fixed point scheme by finding appropriate parameters α and β so that

$$(2.6) \quad \limsup_{k \rightarrow \infty} \|x_k - x_*\|^{1/k} \leq 1 - \sqrt{\epsilon} ,$$

for matrices P with spectral radius bounded by $1 - \epsilon$.

REMARK 1. If P is symmetric, the iteration (2.4) can be recovered by applying the accelerated gradient descent scheme (2.1) to the quadratic function $f(x) \equiv \frac{1}{2}x^\top(I - P)x - g^\top x$. The damping parameter β corresponds to the step h . However, Nesterov's results only apply to the case when f is a strongly convex function. This requires in particular $I - P$ to be symmetric positive definite. In particular all the eigenvalues of P must be real and smaller than 1.

The scheme (2.4) for fixed point iteration has been considered recently by [19, 16]. Moreover, inspired by the momentum method [28, 15] for improving gradient descent, [16] also proposed a momentum fixed point method described as follows:

$$(2.7) \quad x_{k+1} = (1 - \beta)x_k + \beta T(x_k) + \alpha(x_k - x_{k-1}) .$$

Asymptotic rate analysis for (2.4) (2.7) follows from [16] when the spectrum of P is real.

As discussed in the introduction, our main results apply to complex spectra, and also to higher degree of acceleration.

In the scheme (2.4), y_{k+1} is generated from a linear combination of the last two iterates. We now consider the following *Accelerated Value Iteration of degree d (dA-VI)*, in which y_{k+1} is a linear combination of the last d iterates for any $d \geq 2$,

$$(2.8a) \quad x_{k+1} = (1 - \beta)y_k + \beta T(y_k) ,$$

$$(2.8b) \quad y_{k+1} = (1 + \alpha_{d-2} + \dots + \alpha_0)x_{k+1} - \alpha_{d-2}x_k - \dots - \alpha_0x_{k-d+2} .$$

We will show how to select the parameters $\alpha = (\alpha_0, \dots, \alpha_{d-2})$ to obtain an acceleration of order d , in the sense that

$$(2.9) \quad \limsup_{k \rightarrow \infty} \|x_k - x_*\|^{1/k} \leq 1 - \epsilon^{1/d} .$$

REMARK 2. The idea of accelerating the vanilla KM fixed point method by extrapolating a finite number of previous steps goes back to the work of Anderson in 1965 [1]. The algorithm known as Anderson Acceleration (AA) chooses dynamically the extrapolation coefficients, while the coefficients $\alpha = (\alpha_0, \dots, \alpha_{d-2})$ in dA -VI (2.8) remain constant for all the iterations. The theoretical analysis of AA and of its variants is still under development. In particular, the theoretical convergence rate of AA seems to be missing in the literature, except in the special case when T corresponds to the gradient descent mapping of a strongly convex and smooth function [35]. When T takes the form of (2.3), this requires P to be symmetric, see Remark 1. In [40], a modified AA, interleaving KM updates by using safe-guarding steps, is shown to be globally converging, but the convergence rate is not analyzed. As shown later, the d -AVI (2.8) does not need any safe-guard checking and will converge with accelerated asymptotic rate as in (2.9) under some conditions on the spectrum of P .

REMARK 3. The computational cost of one iteration of the classical Value Iteration algorithm (2.5) is $O(n^2)$. In comparison, the computational cost of one iteration of the dA -VI algorithm (2.8) is $O(n(n+d))$. Regarding the space complexity, the classical Value Iteration needs to store two vectors (x_{k+1}, x_k) each of size n , so it needs a $2n$ space of memory. In comparison, the dA -VI algorithm needs to store $d+1$ vectors $(y_{k+1}, x_{k+1}, \dots, x_{k-d+2})$ each of size n , so it needs $(d+1)n$ space of memory. We notice that in practice the degree d that we will use is small (≤ 4), therefore the computational cost of one iteration of dA -VI and its space complexity are similar to the ones of the classical Value Iteration algorithm. Moreover, the asymptotic convergence rate $1 - \epsilon^{1/d}$ allows the dA -VI algorithm to converge in a number of iterations smaller than the Value Iteration algorithm (see the numerical experiments in Section 5).

3. Analysis of Accelerated Value Iteration of degree 2. In this section we analyse the AVI scheme (2.4). We will show that with an appropriate choice of the acceleration parameter α , and under an assumption on the shape of the complex spectrum of P , the asymptotic rate can indeed be improved up to $1 - \sqrt{\epsilon}$. We also show that the damping parameter β will allow us to enlarge the convergence region, while keeping the acceleration properties. We deal separately with the special $d = 2$ case, since it is more elementary, easier to compare with existing acceleration schemes, and since it gives insight on the generalization to the higher degree case which will be done in Section 4.

3.1. The spectrum of the AVI iteration. We define $P_\beta := (1 - \beta)I + \beta P$. Then, the AVI algorithm (2.4) can be written as the second order iteration

$$(3.1) \quad y_{k+1} = \beta g + (1 + \alpha)P_\beta y_k - \alpha P_\beta y_{k-1}.$$

Considering $z_k = y_k - x_*$, the iteration becomes $z_{k+1} = (1 + \alpha)P_\beta z_k - \alpha P_\beta z_{k-1}$. This is equivalent to:

$$(3.2) \quad \begin{pmatrix} z_{k+1} \\ z_k \end{pmatrix} = \begin{pmatrix} (1 + \alpha)P_\beta & -\alpha P_\beta \\ I & 0 \end{pmatrix} \begin{pmatrix} z_k \\ z_{k-1} \end{pmatrix}$$

Without loss of generality we first deal with the case with no damping, i.e., $\beta = 1$. The discussion for general $\beta \in (0, 1]$ can be found in Subsection 3.2. Then, the matrix appearing in (3.2) becomes

$$(3.3) \quad Q_\alpha := \begin{pmatrix} (1 + \alpha)P & -\alpha P \\ I & 0 \end{pmatrix}.$$

The asymptotic rate of convergence of the sequence (z_k) in the system (3.2), when it is converging, and thus of the sequence (y_k) in the AVI scheme (2.4) is determined by the

spectral radius of Q_α . Recall that we want to improve this asymptotic rate, thus it suffices to find appropriate values of α such that the spectral radius of Q_α is as small as possible.

We first relate the eigenvalues of Q_α with those of P . We introduce the following rational function of degree 2, defined on $\mathbb{C} \setminus \{\alpha/(1+\alpha)\}$ by

$$\phi_\alpha(z) := \frac{z^2}{(1+\alpha)z - \alpha}.$$

The following is a standard property of block-companion matrices, we provide the proof for completeness.

LEMMA 3.1. *If $\alpha \neq 0$ then λ is an eigenvalue of Q_α if and only if there exists an eigenvalue δ of P such that $\delta = \phi_\alpha(\lambda)$. In other words,*

$$\text{spec } Q_\alpha = \phi_\alpha^{-1}(\text{spec } P).$$

Proof. Let λ be an eigenvalue of Q_α . There exists a non-zero vector $\begin{pmatrix} z_1 \\ z_0 \end{pmatrix} \in \mathbb{R}^{2n}$ such that $Q_\alpha \begin{pmatrix} z_1 \\ z_0 \end{pmatrix} = \lambda \begin{pmatrix} z_1 \\ z_0 \end{pmatrix}$. This is equivalent to $(1+\alpha)Pz_1 - \alpha Pz_0 = \lambda z_1$ and $z_1 = \lambda z_0$, or equivalently $(\lambda(1+\alpha) - \alpha)Pz_0 = \lambda^2 z_0$ and $z_1 = \lambda z_0$. We have $z_0 \neq 0$, because otherwise $z_1 = \lambda z_0 = 0$. We notice that $\lambda(1+\alpha) - \alpha \neq 0$, because otherwise $\lambda = \frac{\alpha}{1+\alpha} \neq 0$ and $\lambda^2 z_0 = 0$, then $z_0 = 0$, which is not true. Therefore $Pz_0 = \phi_\alpha(\lambda)z_0$ which allows to conclude. \square

3.1.1. The case of real eigenvalues. We now explain how to select α optimally. We first suppose that the spectrum of P is real and nonnegative, i.e., $\text{spec } P \subset [0, 1-\epsilon]$ for some $\epsilon \in (0, 1)$. We denote by $\mathcal{B}(z, r)$ the closed disk of the complex plane with center z and radius r . We consider the minimax problem

$$(3.4) \quad \min_{\alpha > 0} \max_{P: \text{spec } P \subset [0, 1-\epsilon]} \rho(Q_\alpha)$$

where ρ denotes the spectral radius, and the matrix Q_α , depending on P , is defined by (3.3).

LEMMA 3.2. *The solution α^* of the minimax problem (3.4) is given by*

$$(3.5) \quad \alpha^* = \frac{1 - \sqrt{\epsilon}}{1 + \sqrt{\epsilon}}.$$

It guarantees that $\text{spec } Q_{\alpha^} \subset \mathcal{B}(0, 1 - \sqrt{\epsilon})$, for all matrices P such that $\text{spec } P \subset [0, 1 - \epsilon]$.*

Proof. By Lemma 3.1, $\lambda \in \text{spec } Q_\alpha$ if and only if there exists $\delta \in \text{spec } P \subset [0, 1 - \epsilon]$, such that $\delta = \frac{\lambda^2}{(1+\alpha)\lambda - \alpha}$. This can be written as a second degree equation in λ :

$$(3.6) \quad \lambda^2 - (1+\alpha)\delta\lambda + \alpha\delta = 0.$$

The discriminant of this equation is $\Delta = \delta^2(1+\alpha)^2 - 4\alpha\delta = \delta(1+\alpha)^2(\delta - \alpha')$, where $\alpha' := \frac{4\alpha}{(1+\alpha)^2}$. We note that the function $\alpha \mapsto \frac{4\alpha}{(1+\alpha)^2}$ is a strictly increasing bijection from $[0, 1]$ to itself, with inverse function $\alpha \mapsto \frac{1 - \sqrt{1 - \alpha}}{1 + \sqrt{1 - \alpha}}$. Hence $\alpha' \geq 1 - \epsilon$ if and only if $\alpha \geq \alpha^*$.

CLAIM 1. *For fixed α , the maximal modulus of the solutions of (3.6) is increasing with δ .*

Proof of Claim 1. If $\Delta \leq 0$, i.e. $\delta \leq \alpha'$, then the solutions of (3.6) are complex conjugate $\lambda_\pm = \frac{1}{2}(\delta(1+\alpha) \pm i\sqrt{\delta(1+\alpha)^2(\alpha' - \delta)})$, and we have $\lambda_+ \lambda_- = \alpha\delta$. Then $|\lambda_+| = |\lambda_-| = \sqrt{\alpha\delta}$, which is increasing in δ .

If $\Delta \geq 0$, i.e. $\delta \geq \alpha'$, the solutions of (3.6) are real:

$$\lambda_{\pm} = \frac{1}{2}(\delta(1 + \alpha) \pm \sqrt{\delta(1 + \alpha)^2(\delta - \alpha')}).$$

Then $\max(|\lambda_+|, |\lambda_-|) = \frac{1}{2}(\delta(1 + \alpha) + \sqrt{\delta(1 + \alpha)^2(\delta - \alpha')})$ is strictly increasing in δ . \square

Claim 1 shows that

$$(3.7) \quad \max_{P: \text{spec } PC[0, 1-\epsilon]} \rho(Q_\alpha) = \max \{|\lambda| : \lambda^2 - (1 + \alpha)(1 - \epsilon)\lambda + \alpha(1 - \epsilon) = 0.\}$$

The discriminant of the second order equation in (3.7) is

$$\Delta = (1 - \epsilon)^2(1 + \alpha)^2 - 4\alpha(1 - \epsilon) = (1 - \epsilon)(1 + \alpha)^2(1 - \epsilon - \alpha').$$

If $\alpha \geq \alpha^*$, then $\alpha' \geq 1 - \epsilon$ and $\Delta \leq 0$. In this case $|\lambda_+| = |\lambda_-| = \sqrt{\alpha(1 - \epsilon)}$ is increasing in $\alpha \in \left[\frac{1 - \sqrt{\epsilon}}{1 + \sqrt{\epsilon}}, 1\right]$. If $\alpha \leq \alpha^*$, then $\alpha' \leq 1 - \epsilon$ and $\Delta \geq 0$. In this case

$$\max(|\lambda_+|, |\lambda_-|) = \frac{1}{2} \left((1 - \epsilon)(1 + \alpha) + \sqrt{(1 - \epsilon)^2(1 + \alpha)^2 - 4\alpha(1 - \epsilon)} \right).$$

CLAIM 2. The function $F : \alpha \rightarrow (1 - \epsilon)(1 + \alpha) + \sqrt{(1 - \epsilon)^2(1 + \alpha)^2 - 4\alpha(1 - \epsilon)}$ is strictly decreasing on $\left[0, \frac{1 - \sqrt{\epsilon}}{1 + \sqrt{\epsilon}}\right]$.

Proof of Claim 2. We have

$$F'(\alpha) = 1 - \epsilon + \frac{2(1 - \epsilon)^2(1 + \alpha) - 4(1 - \epsilon)}{2\sqrt{(1 - \epsilon)^2(1 + \alpha)^2 - 4\alpha(1 - \epsilon)}} = \frac{(1 - \epsilon)h(\alpha)}{\sqrt{(1 - \epsilon)^2(1 + \alpha)^2 - 4\alpha(1 - \epsilon)}},$$

where $h(\alpha) = \sqrt{(1 - \epsilon)^2(1 + \alpha)^2 - 4\alpha(1 - \epsilon)} + (1 - \epsilon)(1 + \alpha) - 2$. It is easy to check that $h(\alpha) = \sqrt{(2 - (1 - \epsilon)(1 + \alpha))^2 - 4\epsilon} - (2 - (1 - \epsilon)(1 + \alpha)) < 0$ for all $\alpha \in \left[0, \frac{1 - \sqrt{\epsilon}}{1 + \sqrt{\epsilon}}\right]$. Since $2 - (1 - \epsilon)(1 + \alpha) \geq 0$ for all $\alpha \in \left[0, \frac{1 - \sqrt{\epsilon}}{1 + \sqrt{\epsilon}}\right]$, we deduce that $h(\alpha) < 0$ and hence $F'(\alpha) < 0$ for all $\alpha \in \left[0, \frac{1 - \sqrt{\epsilon}}{1 + \sqrt{\epsilon}}\right]$. \square

We conclude that the best choice of α which minimizes the maximum of the spectral radius of Q_α corresponding to all P with spectrum in $[0, 1 - \epsilon]$ is α^* given in (3.5), and it allows to have $\text{spec } Q_{\alpha^*} \subset \mathcal{B}(0, 1 - \sqrt{\epsilon})$ for all such matrix P . \square

REMARK 4. If P is symmetric, then the quadratic function f in Remark 1 is a strongly convex function with $L = 1$ and $\mu = \epsilon$. In this special case the α^* in Lemma 3.2 coincides with the inertial parameter (2.2) in Nesterov's constant-step method. The same choice of step has been proposed, for nonsymmetric matrices with real spectrum, in [19].

3.1.2. The case of complex eigenvalues. Now we do not assume any more that P has a real spectrum. We will show that the best acceleration rate achievable in the case of a real spectrum, obtained by choosing $\alpha = \alpha^*$ as in Lemma 3.2, is still achievable in the case of a complex spectrum satisfying a geometric condition.

Consider the following simple closed curve Γ_ϵ defined by the parametric equation:

$$\theta \mapsto \frac{(1 - \epsilon)e^{2i\theta}}{2e^{i\theta} - 1}, \quad \theta \in (0, 2\pi].$$

Denote by Σ_ϵ the compact set delimited by the curve Γ_ϵ . We show in Figure 3.1 the curve Γ_0 and the enclosed region Σ_0 . It is easy to see that Γ_ϵ (resp. Σ_ϵ) is a scaling of Γ_0 (resp. Σ_0) by $1 - \epsilon$. Moreover, we have

$$(3.8) \quad \left| \frac{e^{2i\theta}}{2e^{i\theta} - 1} \right| = \frac{1}{|2e^{i\theta} - 1|} \leq \frac{1}{|2e^{i\theta}| - 1} = 1,$$

and thus the curve Γ_ϵ is included in the disk $\mathcal{B}(0, 1 - \epsilon)$. It follows that

$$(3.9) \quad \Sigma_\epsilon \subset \mathcal{B}(0, 1 - \epsilon).$$

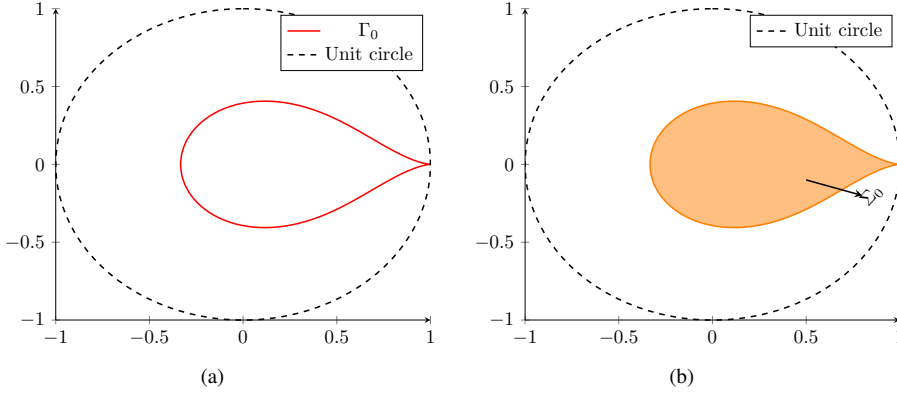


FIGURE 3.1. Illustration of the curve Γ_0 (Figure 3.1(a)) and its enclosed region Σ_0 (Figure 3.1(b)).

THEOREM 3.3. *Let $\epsilon \in (0, 1)$, P be a $n \times n$ complex matrix and Q_α be defined as in (3.3) with $\alpha = (1 - \sqrt{\epsilon})/(1 + \sqrt{\epsilon})$. If $\text{spec } P \subset \Sigma_\epsilon$, then $\text{spec } Q_\alpha \subset \mathcal{B}(0, 1 - \sqrt{\epsilon})$.*

Proof. To show that $\text{spec } P \subset \Sigma_\epsilon \Rightarrow \text{spec } Q_\alpha \subset \mathcal{B}(0, 1 - \sqrt{\epsilon})$, we will prove the contrapositive

$$(3.10) \quad \text{spec } Q_\alpha \cap \mathbb{C} \setminus \mathcal{B}(0, 1 - \sqrt{\epsilon}) \neq \emptyset \Rightarrow \text{spec } P \cap \mathbb{C} \setminus \Sigma_\epsilon \neq \emptyset.$$

We consider an eigenvalue $\lambda \in \text{spec } Q_\alpha \cap \mathbb{C} \setminus \mathcal{B}(0, 1 - \sqrt{\epsilon})$ so that $\lambda = r(1 - \sqrt{\epsilon})e^{i\bar{\theta}}$ for some $\bar{\theta} \in (0, 2\pi]$ and $r > 1$. The associated eigenvalue of P is

$$\delta_r(\bar{\theta}) := \frac{\lambda^2}{(1 + \alpha)\lambda - \alpha} = \frac{(1 - \sqrt{\epsilon})^2 r^2 e^{2i\bar{\theta}}}{\frac{2}{1 + \sqrt{\epsilon}} r(1 - \sqrt{\epsilon}) e^{i\bar{\theta}} - \frac{1 - \sqrt{\epsilon}}{1 + \sqrt{\epsilon}}} = \frac{(1 - \epsilon)r^2 e^{2i\bar{\theta}}}{2r e^{i\bar{\theta}} - 1}.$$

It is easy to check from $r > 1$ that

$$|\delta_r(0)| = \frac{(1 - \epsilon)r^2}{2r - 1} > 1 - \epsilon,$$

which together with (3.9) implies that

$$\delta_r(0) \notin \Sigma_\epsilon.$$

Suppose that $\delta_r(\bar{\theta}) \in \Sigma_\epsilon$. Since the curve Γ_ϵ is the boundary of the compact set Σ_ϵ , there must be a $\theta \in (0, 2\pi)$ such that

$$\delta_r(\theta) \in \Gamma_\epsilon.$$

In other words, there is $u, v \in \mathbb{C}$ such that $|u| = |v| = 1$ and $(1 - \epsilon)\frac{u^2}{2u-1} = (1 - \epsilon)\frac{r^2v^2}{2rv-1}$. Then $r^2(2u-1)v^2 - 2ru^2v + u^2 = 0$. We consider v as the unknown variable in this equation. The discriminant is $\Delta = 4r^2u^2(u-1)^2$ and then

$$v \in \left\{ \frac{2ru^2 \pm 2ru(u-1)}{2r^2(2u-1)} \right\} = \left\{ \frac{u}{r}, \frac{u}{r(2u-1)} \right\}.$$

Since $|u| = |v|$, it is impossible that $v = \frac{u}{r}$. If $v = \frac{u}{r(2u-1)}$, then by taking the module we have $|2u-1| = \frac{1}{r}$, which is absurd because $|2u-1| \geq |2u|-1 = 1 > \frac{1}{r}$. We thus conclude that $\delta_r(\bar{\theta}) \in \mathbb{C} \setminus \Sigma_\epsilon$ and (3.10) is proved. \square

REMARK 5. In Theorem 4.3, we will give an analysis for acceleration of arbitrary degree $d \geq 2$, which recovers Theorem 3.3 for the case $d = 2$ and in addition shows that if $\text{spec } Q_\alpha \subset \mathcal{B}(0, 1 - \sqrt{\epsilon})$, then $\text{spec } P \subset \Sigma_\epsilon$.

For any $r \geq 1$, denote by $\Gamma_\epsilon(r)$ the simple closed curve defined by the parametric equation $\theta \mapsto \delta_r(\theta), \theta \in (0, 2\pi]$, and denote by $\Sigma_\epsilon(r)$ the region enclosed by $\Gamma_\epsilon(r)$. We have the following stronger result.

THEOREM 3.4. Let $\epsilon \in (0, 1)$, P be a $n \times n$ complex matrix, Q_α be defined as in (3.3) with $\alpha = (1 - \sqrt{\epsilon})/(1 + \sqrt{\epsilon})$ and $r \geq 1$. If $\text{spec } P \subset \Sigma_\epsilon(r)$, then $\text{spec } Q_\alpha \subset \mathcal{B}(0, r(1 - \sqrt{\epsilon}))$.

An ingredient of the proof of Theorem 3.3 was to show that for any $r > 1$, the curve $\Gamma_\epsilon(r)$ does not intersect with the curve Γ_ϵ . In a similar way, we can prove the above Theorem 3.4, by showing that the curve $\Gamma_\epsilon(r)$ does not intersect with the curve $\Gamma_\epsilon(r')$ for any distinct $r \geq 1$ and $r' \geq 1$.

REMARK 6. Let $0 < \gamma \leq 1$. An equivalent statement of Theorem 3.4 is as follows: if $\text{spec } P \subset \Sigma_\epsilon \left(\frac{1 - \gamma\sqrt{\epsilon}}{1 - \sqrt{\epsilon}} \right)$, then $\text{spec } Q_\alpha \subset \mathcal{B}(0, 1 - \gamma\sqrt{\epsilon})$. This implies that the asymptotic rate can be of order $1 - \Omega(\sqrt{\epsilon})$ if the spectrum of P is sufficiently close to Σ_ϵ . We illustrate this result in Figure 3.2 with the example of $\epsilon = 0.01$ and $\gamma = 0.5$.

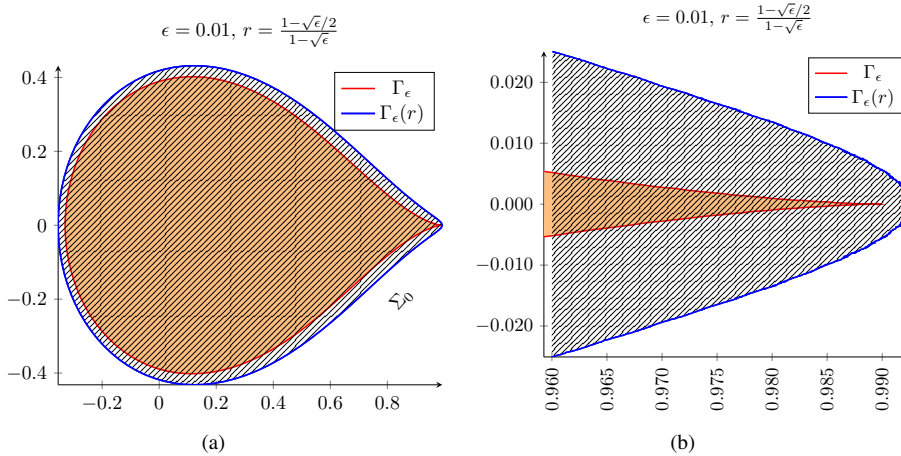


FIGURE 3.2. Illustration of the curve Γ_ϵ (the curve in red) and its enclosed region Σ_ϵ (the region in orange), and the curve $\Gamma_\epsilon(r)$ (the curve in blue) and its enclosed region $\Sigma_\epsilon(r)$ (the dashed region). Figure 3.2(a) is a zoom of Figure 3.2(b).

3.2. Enlargement of the accelerable region by damping. In this subsection we consider the effect of the Krasnosel'skiĭ-Mann damping parameter $\beta \in (0, 1]$. The following corollary, which is immediate from [Theorem 3.3](#), determines the accelerable region for the spectrum of the initial matrix P .

COROLLARY 3.5. *If there is $\beta \in (0, 1]$ such that $\text{spec } P_\beta \subset \Sigma_\epsilon$, then AVI algorithm (2.4) with the parameters β and $\alpha = \frac{1-\sqrt{\epsilon}}{1+\sqrt{\epsilon}}$ converges with an asymptotic rate no greater than $1 - \sqrt{\epsilon}$, i.e., (2.6) holds.*

Based on [Corollary 3.5](#), we now look for a radius $r > 0$ such that if $\text{spec } P \subset \mathcal{B}(0, r) \cup [-1 + \epsilon, 1 - \epsilon]$, then there is a scaling parameter $\beta \in (0, 1]$ such that $\text{spec } P_\beta \subset \Sigma_{\epsilon'}$, for some $\epsilon' > 0$, with the goal of achieving an accelerated asymptotic rate $1 - \Omega(\sqrt{\epsilon})$.

We start by giving a disk and a part of the real line which are contained in Σ_0 .

LEMMA 3.6. *We have*

$$\mathcal{B}\left(\frac{1}{3}, \frac{1}{3}\right) \cup \left[-\frac{1}{3}, 1\right] \subset \Sigma_0.$$

Proof. The boundary of Σ_0 intersects with the real axis at $(1, 0)$ and $(-1/3, 0)$. Thus $[-\frac{1}{3}, 1] \subset \Sigma_0$. For any $\theta \in (0, 2\pi]$, we have

$$\begin{aligned} & \left| \frac{e^{2i\theta}}{2e^{i\theta} - 1} - \frac{1}{3} \right|^2 - \frac{1}{9} = \left| \frac{3e^{2i\theta} - 2e^{i\theta} + 1}{3(2e^{i\theta} - 1)} \right|^2 - \frac{1}{9} \\ &= \frac{|3e^{2i\theta} - 2e^{i\theta} + 1|^2 - |2e^{i\theta} - 1|^2}{9|2e^{i\theta} - 1|^2} \\ &= \frac{14 - 16 \cos(\theta) + 6 \cos(2\theta) - 5 + 4 \cos(\theta)}{9|2e^{i\theta} - 1|^2} \\ &= \frac{4 \cos^2(\theta) - 4 \cos(\theta) + 1}{9|2e^{i\theta} - 1|^2} = \frac{(2 \cos(\theta) - 1)^2}{9|2e^{i\theta} - 1|^2} \geq 0. \end{aligned}$$

Thus the boundary of Σ_0 does not intersect the interior of the disk $\mathcal{B}(\frac{1}{3}, \frac{1}{3})$. Since $0 \in \Sigma_0 \cap \mathcal{B}(\frac{1}{3}, \frac{1}{3})$, the disk $\mathcal{B}(\frac{1}{3}, \frac{1}{3})$ is entirely contained in Σ_0 . \square

The following result shows that if the spectrum of the initial matrix P belongs to a ‘‘flying saucer’’ shaped region of the complex plane (see [Figure 3.3\(a\)](#) for illustration), the AVI algorithm does converge with an asymptotic rate $1 - \Omega(\sqrt{\epsilon})$.

THEOREM 3.7. *If $\text{spec } P \subset \mathcal{B}(0, \frac{1-\epsilon}{2}) \cup [-1 + \epsilon, 1 - \epsilon]$, then by setting $\beta = \frac{2}{3-\epsilon}$ and*

$$(3.11) \quad \alpha = \frac{1 - \sqrt{2\epsilon/(3-\epsilon)}}{1 + \sqrt{2\epsilon/(3-\epsilon)}},$$

the iterates of algorithm AVI (2.4) satisfy

$$\limsup_{k \rightarrow \infty} \|x_k - x_*\|^{1/k} \leq 1 - \sqrt{\frac{2\epsilon}{3}}.$$

Proof. For any $\beta \in (0, 1]$, the spectrum of P_β is the image of the spectrum of P by the homothety $H^\beta := z \mapsto 1 - \beta + \beta z$ of center 1 and ratio β . Note that $\beta = \frac{2}{3-\epsilon}$ satisfies

$$1 - \beta = \frac{\beta(1 - \epsilon)}{2} = \frac{1 - \beta\epsilon}{3}.$$

Hence the image of $\mathcal{B}(0, \frac{1-\epsilon}{2}) \cup [-1 + \epsilon, 1 - \epsilon]$ by the homothety H^β is

$$\mathcal{B}\left(\frac{1-\beta\epsilon}{3}, \frac{1-\beta\epsilon}{3}\right) \cup \left[-\frac{1-\beta\epsilon}{3}, 1-\beta\epsilon\right].$$

See [Figure 3.3\(b\)](#) for an illustration. In view of [Lemma 3.6](#), this region is contained in $\Sigma_{\beta\epsilon}$. It follows that $\text{spec } P_\beta \subset \Sigma_{\beta\epsilon}$ and the statement follows by applying [Corollary 3.5](#). \square

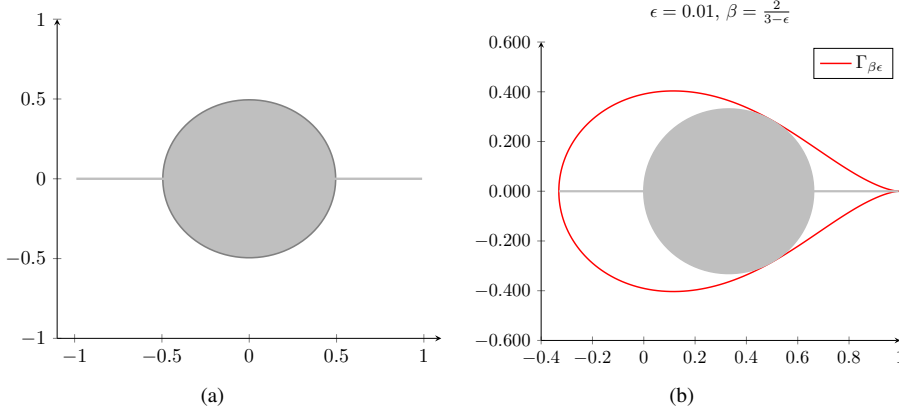


FIGURE 3.3. (a): the region $\mathcal{B}(0, \frac{1-\epsilon}{2}) \cup [-1 + \epsilon, 1 - \epsilon]$ (the flying saucer shaped region in grey). (b): the curve $\Sigma_{\beta\epsilon}$ (the curve in red) and the image of $\mathcal{B}(0, \frac{1-\epsilon}{2}) \cup [-1 + \epsilon, 1 - \epsilon]$ by the homothety H^β .

REMARK 7. For $0 < \epsilon < \frac{1}{3}$, the flying saucer shaped region $\mathcal{B}(0, \frac{1-\epsilon}{2}) \cup [-1 + \epsilon, 1 - \epsilon]$ can not be included in Σ_0 and [Corollary 3.5](#) is not applicable. However, the homothety H^β with $\beta = \frac{2}{3-\epsilon}$ sends this region inside $\Sigma_{\beta\epsilon}$, whence an accelerated asymptotic rate.

REMARK 8. In the special case when $\text{spec } P \subset [-1 + \epsilon, 1 - \epsilon]$, a similar result was established in [16]. Translated with our notations, Theorem 5.1 in [16] proved an asymptotic rate $1 - \sqrt{\epsilon/(2-\epsilon)}$ by setting $\alpha = 1/(2-\epsilon)$ and $\beta = \frac{1-\sqrt{\epsilon/(2-\epsilon)}}{1+\sqrt{\epsilon/(2-\epsilon)}}$ in (2.4).

We complement [Theorem 3.7](#) by showing the optimality of the radius $\frac{1-\epsilon}{2}$ in the sense described by the following lemma.

LEMMA 3.8. *The largest radius $r \geq 0$, for which there exists $\beta \in (0, 1]$ such that $H^\beta(\mathcal{B}(0, r)) \subset \Sigma_0$, is $r = \frac{1}{2}$ and it corresponds to the choice $\beta = \frac{2}{3}$.*

Proof. Applying the homothety H^β to $\mathcal{B}(0, r)$ leads to the ball $\mathcal{B}(1-\beta, \beta r)$. We thus look for the largest r such that $\mathcal{B}(1-\beta, \beta r) \subset \Sigma_0$ for some $\beta \in (0, 1)$. We notice that $r > 1$ is not possible, because for any $r > 1$ we have $1 + \beta(r-1) > 1$, which is outside Σ_0 .

Now, we suppose that $0 \leq r \leq 1$ and there is $\beta \in (0, 1)$ such that $\mathcal{B}(1-\beta, \beta r) \subset \Sigma_0$. We consider the line (D_r) of the complex plane passing through the point of coordinates $(1, 0)$ and tangent to the upper half of the circle $\mathcal{B}(0, r)$. This line is given by the equation

$$y = \frac{r}{\sqrt{1-r^2}}(1-x).$$

Note that (D_r) is invariant by the homothety H^β and thus is also tangent to $\mathcal{B}(1-\beta, \beta r)$. Thus (D_r) must intersect with Σ_0 at a point other than $(1, 0)$, see [Figure 3.4](#) for an illustration.

The curve Γ_0 is given by

$$\theta \mapsto \frac{e^{2i\theta}}{2e^{i\theta} - 1} = \frac{2 \cos(\theta) - \cos(2\theta)}{5 - 4 \cos(\theta)} + i \frac{2 \sin(\theta) - \sin(2\theta)}{5 - 4 \cos(\theta)}, \quad \theta \in (0, 2\pi].$$

Let $\theta \in (0, 2\pi)$ such that $(x_0, y_0) := \left(\frac{2 \cos(\theta) - \cos(2\theta)}{5 - 4 \cos(\theta)}, \frac{2 \sin(\theta) - \sin(2\theta)}{5 - 4 \cos(\theta)} \right)$ lies in $(D_r) \cap \Sigma_0$.

Then

$$\frac{r}{\sqrt{1-r^2}} = \frac{y_0}{1-x_0} = \frac{2 \sin(\theta)(1 - \cos(\theta))}{5 - 6 \cos(\theta) + 2 \cos^2(\theta) - 1} = \frac{\sin(\theta)}{2 - \cos(\theta)}.$$

We can easily prove that:

$$\max_{\theta \in (0, 2\pi)} \frac{\sin(\theta)}{2 - \cos(\theta)} = \frac{\sqrt{3}}{3}.$$

Hence,

$$\frac{r}{\sqrt{1-r^2}} \leq \frac{\sqrt{3}}{3},$$

which implies that $r \leq 1/2$.

When $r = 1/2$, we let $\beta = 2/3$. Then the image of $\mathcal{B}(0, r)$ by the homothety H^β is $\mathcal{B}(1/3, 1/3)$, which by [Lemma 3.6](#) is contained in Σ_0 . \square

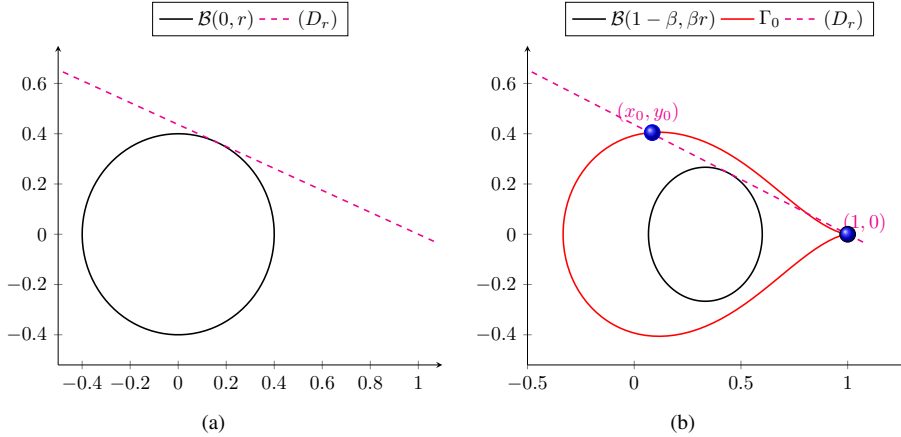


FIGURE 3.4. (a): the line (D_r) is tangent to the boundary of $\mathcal{B}(0, r)$. (b): the line (D_r) is tangent to the boundary of $\mathcal{B}(1 - \beta, \beta r)$, which is contained in Σ_0 . The line (D_r) intersects Σ_0 at $(1, 0)$ and (x_0, y_0) .

4. Analysis of Accelerated Value Iteration of degree d . In this section we consider the acceleration scheme dA -VI (2.8) of any order $d \geq 2$. Hereinafter, $\alpha = (\alpha_0, \dots, \alpha_{d-2}) \in \mathbb{R}^{d-1}$ denotes the vector of parameters required in (2.8b). We shall extend the previous results for $d = 2$ to arbitrary $d \geq 2$. That is, with an appropriate choice of α , and under an assumption on the shape of the complex spectrum of P , the asymptotic rate of (2.8) can be $1 - \epsilon^{1/d}$. We refer to Remark 2 for a discussion on the connection between the dA -VI (2.8) and Anderson acceleration.

4.1. Parameters. We show how to select the parameters $\alpha = (\alpha_0, \dots, \alpha_{d-2})$ in (2.8b) to obtain an acceleration of any order $d \geq 2$. For the sake of simplicity we let $\beta = 1$. Then

$z_k = y_k - x_*$ satisfies the following system of linear equations:

$$\begin{pmatrix} z_{k+1} \\ z_k \\ \vdots \\ z_{k-d+2} \end{pmatrix} = Q_{\alpha,d} \begin{pmatrix} z_k \\ z_{k-1} \\ \vdots \\ z_{k-d+1} \end{pmatrix}$$

where

$$Q_{\alpha,d} := \begin{pmatrix} (1 + \alpha_{d-2} + \cdots + \alpha_0)P & -\alpha_{d-2}P & \cdots & -\alpha_0P \\ I & 0 & \cdots & 0 \\ \vdots & \ddots & & \vdots \\ 0 & \cdots & I & 0 \end{pmatrix},$$

We introduce the following rational function of degree d defined by

$$(4.1) \quad \phi_{\alpha,d}(\lambda) = \frac{\lambda^d}{U(\lambda)},$$

where $U(\cdot) : \mathbb{C} \rightarrow \mathbb{C}$ is the polynomial of degree $d - 1$ given by:

$$U(\lambda) = (1 + \alpha_{d-2} + \cdots + \alpha_0)\lambda^{d-1} - \alpha_{d-2}\lambda^{d-2} - \cdots - \alpha_0.$$

The polynomial U satisfies $U(1) = 1$. The following standard result, which is proved as [Lemma 3.1](#) above, relates the eigenvalues of $Q_{\alpha,d}$ with those of P .

LEMMA 4.1. λ is an eigenvalue of Q_{α} if and only if there exists an eigenvalue δ of P such that $\delta = \phi_{\alpha,d}(\lambda)$. In other words,

$$\text{spec } Q_{\alpha,d} = \phi_{\alpha,d}^{-1}(\text{spec } P).$$

We want to choose the vector of parameters α that leads to the smallest possible spectral radius for $Q_{\alpha,d}$, in order to obtain the smallest asymptotic rate for (2.8), like in the case of AVI (i.e. $d = 2$).

LEMMA 4.2. The best choice of the parameters $\alpha_0, \dots, \alpha_{d-2}$ that minimizes the maximum of the moduli of the preimages of $1 - \epsilon$ by $\phi_{\alpha,d}$ is:

$$(4.2) \quad \alpha_i = \binom{d}{i} \frac{(\epsilon^{1/d} - 1)^{d-i}}{(1 - \epsilon)}, \quad \forall i = 0, \dots, d-2,$$

and it corresponds to the following rational function

$$(4.3) \quad \phi_d^*(\lambda) = \frac{(1 - \epsilon)\lambda^d}{\lambda^d - (\lambda - (1 - \epsilon^{1/d}))^d}.$$

Proof. It is easy to verify that with the choice of $\alpha_0, \dots, \alpha_{d-2}$ in (4.2),

$$U(\lambda) = \frac{1}{1 - \epsilon} \left(\lambda^d - (\lambda - (1 - \epsilon^{1/d}))^d \right),$$

and thus it leads to the rational function (4.3). In addition, $\phi_d^*(\lambda) = 1 - \epsilon$ if and only if $(\lambda - (1 - \epsilon^{1/d}))^d = 0$, from which we deduce that the maximal moduli of the preimages of $1 - \epsilon$ by ϕ_d^* is $1 - \epsilon^{1/d}$.

Let $\lambda_1, \lambda_2, \dots, \lambda_d$ be the solutions of $\phi_{\alpha,d}(\lambda) = 1 - \epsilon$ satisfying $\max_i |\lambda_i| \leq 1 - \epsilon^{1/d}$. Then $\lambda^d - (1 - \epsilon)U(\lambda) = \prod_i (\lambda - \lambda_i)$ for all $\lambda \in \mathbb{C}$. By taking $\lambda = 1$ we obtain that $\prod_i (1 - \lambda_i) = \epsilon$. We have

$$\epsilon \leq (1 - \max_i |\lambda_i|)^d \leq \prod_i (1 - |\lambda_i|) \leq \prod_i |1 - \lambda_i| = \epsilon .$$

Therefore for all i , $\lambda_i = 1 - \epsilon^{1/d}$ and $\phi_{\alpha,d}$ is exactly ϕ_d^* . \square

In the following, we consider the scheme (2.8) implemented with the special choice of the parameters $\{\alpha_i : i = 0, \dots, d-2\}$ given in (4.2). We want to generalize the characterization of the accelerable region Σ_ϵ for the AVI algorithm to get the largest accelerable region for the dA -VI algorithm. For this purpose, for any $\epsilon \geq 0$ and $d \geq 2$, let $\Gamma_{\epsilon,d}$ be the simple closed curve defined by the parametric equation:

$$(4.4) \quad \theta \mapsto \frac{(1 - \epsilon)e^{id\theta}}{e^{id\theta} - (e^{i\theta} - 1)^d}, \quad \theta \in \left(\pi - \frac{2\pi}{d}, \pi + \frac{2\pi}{d} \right) .$$

See an illustration in Figure 4.1 for $\epsilon = 0$ and $d = 4$. Denote by $\Sigma_{\epsilon,d}$ the compact set

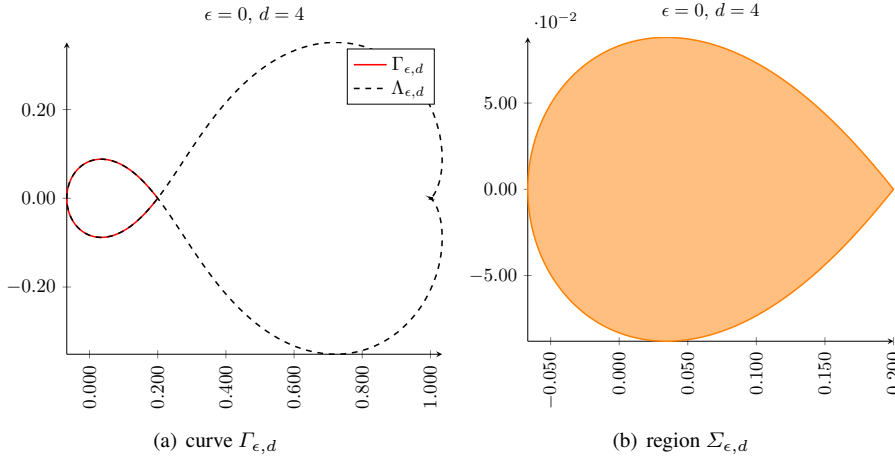


FIGURE 4.1. Illustration of the curve $\Gamma_{\epsilon,d}$ (the curve in red in Figure 4.1(a)) and its enclosed region $\Sigma_{\epsilon,d}$ (Figure 4.1(b)). The dashed curve in Figure 4.1(a) corresponds to $\left\{ \frac{(1-\epsilon)e^{id\theta}}{e^{id\theta} - (e^{i\theta} - 1)^d} : \theta \in (0, 2\pi] \right\}$.

delimited by the simple closed curve $\Gamma_{\epsilon,d}$. The following theorem identifies conditions on the spectrum of the initial matrix P which guarantee that the dA -VI algorithm converges asymptotically with a rate $1 - \epsilon^{1/d}$.

THEOREM 4.3. *Choosing the parameters $(\alpha_0, \dots, \alpha_{d-1})$ as in (4.2), we get that*

$$\text{spec } Q_{\alpha,d} \subset \mathcal{B}(0, 1 - \epsilon^{1/d}),$$

if and only if $\text{spec } P \subset \Sigma_{\epsilon,d} \cup \{1 - \epsilon\}$.

The proof is given in the next subsection.

4.2. Proof of Theorem 4.3.

LEMMA 4.4. $\text{spec } Q_{\alpha,d} \subset \mathcal{B}(0, 1 - \epsilon^{1/d})$ if and only if

$$(4.5) \quad \text{spec } P \subset \{(1 - \epsilon)z : \psi_d^{-1}(z) \subset \mathcal{B}(0, 1)\} ,$$

where ψ_d is the rational function defined by

$$\psi_d(\lambda) = \frac{\lambda^d}{\lambda^d - (\lambda - 1)^d} .$$

Proof. We note from Lemma 4.1 that $\text{spec } Q_{\alpha,d} \subset \mathcal{B}(0, 1 - \epsilon^{1/d})$ if and only if

$$(4.6) \quad \text{spec } P \subset \{z : (\phi_d^*)^{-1}(z) \subset \mathcal{B}(0, 1 - \epsilon^{1/d})\} .$$

We note the following property:

$$(4.7) \quad \phi_d^*((1 - \epsilon^{1/d})\lambda) = \frac{(1 - \epsilon)\lambda^d}{\lambda^d - (\lambda - 1)^d} = (1 - \epsilon)\psi_d(\lambda) ,$$

Hence (4.6) is equivalent to (4.5). □

We next give a description of the following set.

$$(4.8) \quad \mathcal{S} := \{z \in \mathbb{C} : \psi_d^{-1}(z) \subset \mathcal{B}(0, 1)\} .$$

We shall need to define

$$\mathcal{Q} := \bigcap_{k=0}^{d-1} e^{\frac{2k\pi i}{d}} H ,$$

where

$$H := \{w \in \mathbb{C} : \text{Re}(w) \leq 1/2\} ,$$

is the half-plane containing all the complex numbers with real part smaller than 1/2, and $e^{\alpha i}H$ denotes the halfspace obtained by rotating H of angle α .

LEMMA 4.5.

$$(4.9) \quad \mathcal{S} = \left\{ \frac{1}{1 - \frac{1}{z^d}} : z \in \mathcal{Q} \right\} \cup \{1\} .$$

Proof. We define two self-maps of the extended complex plane $\bar{\mathbb{C}}$:

$$(4.10) \quad f_1(\lambda) := \frac{\lambda}{\lambda - 1} ,$$

$$(4.11) \quad f_2(\lambda) := \lambda^d .$$

Note that

$$f_1(\lambda) = 1 + \frac{1}{\lambda - 1} ,$$

which entails that f_1 is an inversion of center 1. In particular, $f_1 \circ f_1(\lambda) = \lambda$ for any $\lambda \in \bar{\mathbb{C}}$. It is easy to see that

$$(4.12) \quad \psi_d(\lambda) = f_1 \circ f_2 \circ f_1(\lambda), \quad \forall \lambda \in \bar{\mathbb{C}} .$$

Hence we know that

$$\begin{aligned}
(4.13) \quad \mathcal{S} &= \{z \in \mathbb{C} : \psi_d^{-1}(z) \subset \mathcal{B}(0, 1)\} \\
&= \{z \in \mathbb{C} : f_1^{-1}(f_2^{-1}(f_1^{-1}(z))) \subset \mathcal{B}(0, 1)\} \\
&= \{z \in \mathbb{C} : f_2^{-1}(f_1^{-1}(z)) \subset f_1(\mathcal{B}(0, 1))\} \\
&= \{f_1(w) \in \mathbb{C} : f_2^{-1}(w) \subset f_1(\mathcal{B}(0, 1))\},
\end{aligned}$$

where the second equality used (4.12), the third equality relies on the bijection property of f_1 and the last equality applies the change of variable $w = f_1^{-1}(z)$.

Now we characterize the set $f_1(\mathcal{B}(0, 1))$. Note that $z = f_1(w)$ if and only if $\frac{1}{z} + \frac{1}{w} = 1$. Thus there is $w \in \mathcal{B}(0, 1)$ such that $z = f_1(w)$ if and only if $|1 - \frac{1}{z}| \geq 1$. We then deduce that

$$(4.14) \quad f_1(\mathcal{B}(0, 1)) = \{w \in \bar{\mathbb{C}} : |w - 1| \geq |w|\}.$$

Note that

$$\{w \in \mathbb{C} : |w - 1| \geq |w|\} = \{w \in \mathbb{C} : \operatorname{Re}(w) \leq 1/2\} = H.$$

Indeed, it is known that a circle passing through the center of an inversion is sent to a line by this inversion, and the disk delimited by the circle is sent to a half-plane. We conclude that

$$(4.15) \quad f_1(\mathcal{B}(0, 1)) = H \cup \{\infty\}.$$

Plugging (4.15) into (4.13) we obtain

$$(4.16) \quad \mathcal{S} = \{f_1(w) \in \mathbb{C} : f_2^{-1}(w) \subset H \cup \{\infty\}\}.$$

It remains to characterize the set

$$\{w \in \bar{\mathbb{C}} : f_2^{-1}(w) \subset H \cup \{\infty\}\} = \{w \in \mathbb{C} : f_2^{-1}(w) \subset H\} \cup \{\infty\}.$$

Define:

$$(4.17) \quad \bar{\mathcal{Q}} := \{z \in \mathbb{C} : f_2^{-1}(f_2(z)) \subset H\}.$$

It is easy to see that:

$$\{w \in \mathbb{C} : f_2^{-1}(w) \subset H\} = \{f_2(z) : z \in \bar{\mathcal{Q}}\}$$

It follows that

$$(4.18) \quad \{w \in \bar{\mathbb{C}} : f_2^{-1}(w) \subset H \cup \{\infty\}\} = \{f_2(z) : z \in \bar{\mathcal{Q}}\} \cup \{\infty\}.$$

Finally plugging (4.18) into (4.16) we obtain that

$$(4.19) \quad \mathcal{S} = \{f_1(f_2(z)) \in \mathbb{C} : z \in \bar{\mathcal{Q}}\} \cup \{1\} = \left\{ \frac{1}{1 - \frac{1}{z^d}} : z \in \bar{\mathcal{Q}} \right\} \cup \{1\}.$$

Since for any $z \in \mathbb{C}$,

$$f_2^{-1}(f_2(z)) = \left\{ z, e^{-\frac{2\pi i}{d}} z, \dots, e^{-\frac{2(d-1)\pi i}{d}} z \right\},$$

we obtain

$$(4.20) \quad \bar{\mathcal{Q}} = \left\{ z \in \mathbb{C} : \left\{ z, e^{-\frac{2\pi i}{d}} z, \dots, e^{-\frac{2(d-1)\pi i}{d}} z \right\} \subset H \right\}.$$

Therefore, $\bar{\mathcal{Q}}$ is actually the intersection of d halfspaces obtained by rotating H of angles $\frac{2k\pi}{d}$ for $k = 0, \dots, d-1$. Namely,

$$\bar{\mathcal{Q}} = \mathcal{Q}.$$

□

REMARK 9. For $d = 2$, \mathcal{Q} is the set of complex numbers with real part in $[-1/2, 1/2]$. For $d \geq 3$, \mathcal{Q} is a regular polygon with d vertices which circumscribes the disk $\mathcal{B}(0, 1/2)$, see Figure 4.2 for illustration from $d = 2$ to $d = 5$. In particular we have $\mathcal{B}(0, 1/2) \subset \mathcal{Q} \subset \mathcal{B}(0, 1/(2 \cos(\pi/d)))$ and \mathcal{Q} asymptotically approximates $\mathcal{B}(0, 1/2)$ when $d \rightarrow +\infty$. It follows that

$$\left\{ \frac{1}{1 - \frac{1}{z^d}} : z \in \mathcal{B}(0, 1/2) \right\} \cup \{1\} \subset \mathcal{S} \subset \left\{ \frac{1}{1 - \frac{1}{z^d}} : z \in \mathcal{B}(0, 1/(2 \cos(\pi/d))) \right\} \cup \{1\} .$$

Note that for any $a > 1$,

$$\left\{ \frac{1}{1 - \frac{1}{z^d}} : z \in \mathcal{B}(0, a) \right\} = \left\{ \frac{1}{1 - \frac{1}{w}} : w \in \mathcal{B}(0, a^d) \right\} = \left\{ \frac{1}{z} : |z - 1| \geq a^d \right\} .$$

and thus,

$$\mathcal{B}(0, 1/(a^d + 1)) \subset \left\{ \frac{1}{1 - \frac{1}{z^d}} : z \in \mathcal{B}(0, a) \right\} \subset \mathcal{B}(0, 1/(a^d - 1)) .$$

This allows to deduce the following estimation of the region \mathcal{S} .

$$(4.21) \quad \mathcal{B}\left(0, \frac{1}{2^d + 1}\right) \cup \{1\} \subset \mathcal{S} \subset \mathcal{B}\left(0, \frac{1}{(2 \cos(\pi/d))^d - 1}\right) \cup \{1\} .$$

Next we characterize the boundary of the accelerable region \mathcal{S} . We denote by $\text{Bd } S$ the boundary of a set S .

PROPOSITION 4.6. *We have*

$$(4.22) \quad \mathcal{S} = \Sigma_{0,d} \cup \{1\}$$

where $\Sigma_{0,d}$ is the compact set of the complex plane delimited by the simple closed curve $\Gamma_{0,d}$ as defined in (4.4).

Proof. Since f_2 is holomorphic and thus open, it sends the interior of \mathcal{Q} into the interior of $f_2(\mathcal{Q})$. It follows that $\text{Bd } f_2(\mathcal{Q}) \subset f_2(\text{Bd } \mathcal{Q})$. By the continuity of f_2 , for any $z \in \text{Bd } \mathcal{Q}$ and any $\epsilon > 0$, there is $\delta > 0$ such that

$$f_2(\mathcal{B}(z, \delta)) \subset \mathcal{B}(f_2(z), \epsilon) .$$

Since $z \in \text{Bd } \mathcal{Q}$, $\mathcal{B}(z, \delta) \cap \mathcal{Q}^c \neq \emptyset$ and thus $f_2(\mathcal{B}(z, \delta)) \cap f_2(\mathcal{Q}^c) \neq \emptyset$. We note from the definition (4.20) that

$$f_2(\mathcal{Q}) \cap f_2(\mathcal{Q}^c) = \emptyset .$$

Thereby $f_2(\mathcal{B}(z, \delta)) \cap (f_2(\mathcal{Q}))^c \neq \emptyset$ and $\mathcal{B}(f_2(z), \epsilon) \cap (f_2(\mathcal{Q}))^c \neq \emptyset$. This shows that $f_2(z) \in \text{Bd}(f_2(\mathcal{Q}))$ and thus $f_2(\text{Bd } \mathcal{Q}) \subset \text{Bd } f_2(\mathcal{Q})$. We thus proved that

$$(4.23) \quad \text{Bd } f_2(\mathcal{Q}) = f_2(\text{Bd } \mathcal{Q}) .$$

Since $f_1 : \bar{\mathbb{C}} \rightarrow \bar{\mathbb{C}}$ is a homeomorphism, we know that

$$(4.24) \quad \text{Bd } f_1(f_2(\mathcal{Q})) = f_1(\text{Bd } f_2(\mathcal{Q})) \stackrel{(4.23)}{=} f_1(f_2(\text{Bd } \mathcal{Q})) .$$

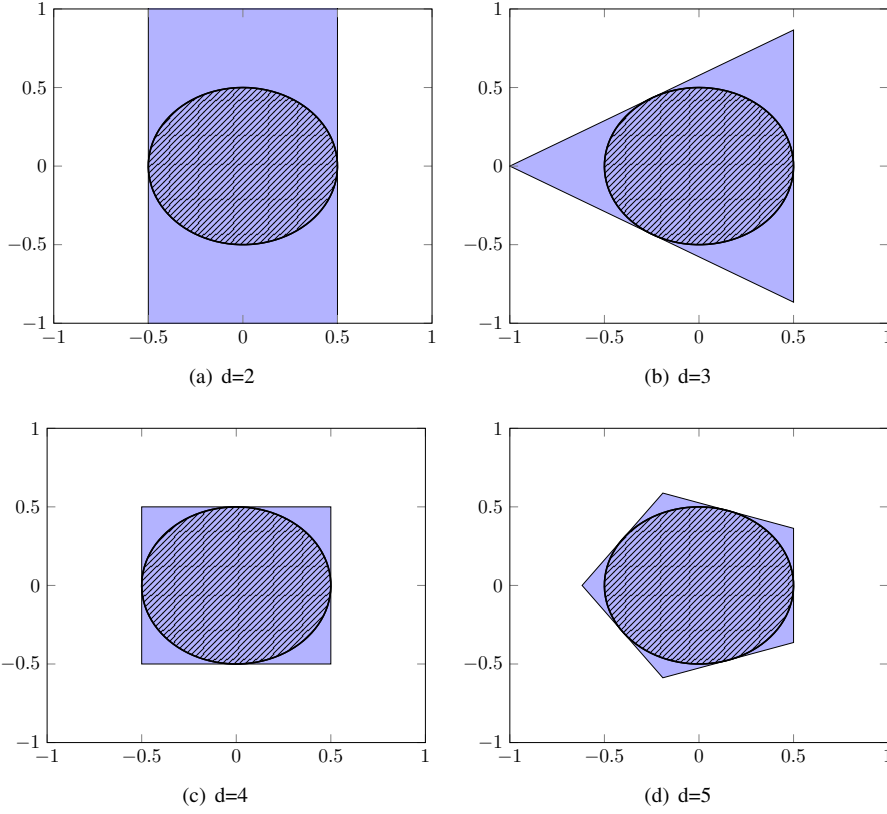


FIGURE 4.2. Illustration of \mathcal{Q} (the region in blue) and the circumscribed disk $\mathcal{B}(0, 1/2)$ (the dashed region).

As mentioned in Remark 9, for $d = 2$, \mathcal{Q} is the set of complex numbers with real part in $[-1/2, 1/2]$ and the boundary of \mathcal{Q} can be described as follows:

$$\text{Bd } \mathcal{Q} = \left\{ \frac{\pm(1 + i \tan \theta)}{2} : \theta \in \left(-\frac{\pi}{2}, \frac{\pi}{2} \right) \right\}.$$

For $d \geq 3$, \mathcal{Q} is the regular convex polygon with boundary given by the simple closed curve:

$$\text{Bd } \mathcal{Q} = \left\{ \frac{e^{\frac{2k\pi i}{d}} (1 + i \tan \theta)}{2} : \theta \in \left(-\frac{\pi}{d}, \frac{\pi}{d} \right], k \in \{0, \dots, d-1\} \right\}.$$

Since

$$\begin{aligned} \frac{1}{1 - e^{-i\theta}} &= \frac{1}{1 - \cos \theta + i \sin \theta} = \frac{1 - \cos \theta - i \sin \theta}{2 - 2 \cos \theta} \\ &= \frac{1}{2} - \frac{i \sin \theta}{2(1 - \cos \theta)} = \frac{1}{2} + \frac{i \sin(\theta + \pi)}{2(1 + \cos(\theta + \pi))} \\ &= \frac{(1 + i \tan \frac{\theta + \pi}{2})}{2}, \end{aligned}$$

we obtain another representation of $\text{Bd } \mathcal{Q}$:

$$(4.25) \quad \text{Bd } \mathcal{Q} = \begin{cases} \left\{ \frac{\pm 1}{1-e^{-i\theta}} : \theta \in (0, 2\pi) \right\} & \text{if } d = 2 \\ \left\{ \frac{e^{\frac{2k\pi i}{d}}}{1-e^{-i\theta}} : \theta \in \left(\pi - \frac{2\pi}{d}, \pi + \frac{2\pi}{d}\right], k \in \{0, \dots, d-1\} \right\}, & \text{if } d \geq 3 \end{cases}$$

Plugging (4.25) into (4.24) we obtain that

$$(4.26) \quad \text{Bd } f_1(f_2(\mathcal{Q})) = \begin{cases} \left\{ \frac{1}{1-(1-e^{-i\theta})^2} : \theta \in (0, 2\pi) \right\} & \text{if } d = 2 \\ \left\{ \frac{1}{1-(1-e^{-i\theta})^d} : \theta \in \left(\pi - \frac{2\pi}{d}, \pi + \frac{2\pi}{d}\right] \right\} & \text{if } d \geq 3 \end{cases}$$

Therefore, define the set

$$(4.27) \quad \Sigma_{0,d} := \begin{cases} f_1(f_2(\mathcal{Q})) \cup \{1\} & \text{if } d = 2 \\ f_1(f_2(\mathcal{Q})) & \text{if } d \geq 3 \end{cases}$$

Then we have (4.22) and

$$(4.28) \quad \text{Bd } \Sigma_{0,d} = \begin{cases} \left\{ \frac{1}{1-(1-e^{-i\theta})^2} : \theta \in (0, 2\pi] \right\} & \text{if } d = 2 \\ \left\{ \frac{1}{1-(1-e^{-i\theta})^d} : \theta \in \left(\pi - \frac{2\pi}{d}, \pi + \frac{2\pi}{d}\right] \right\} & \text{if } d \geq 3 \end{cases}$$

which can be written as

$$\text{Bd } \Sigma_{0,d} = \left\{ \frac{e^{id\theta}}{e^{id\theta} - (e^{i\theta} - 1)^d}, \quad \theta \in \left(\pi - \frac{2\pi}{d}, \pi + \frac{2\pi}{d}\right] \right\}.$$

for any $d \geq 2$. Finally the compactness of $\Sigma_{0,d}$ follows from the compactness of \mathcal{S} , which can be easily seen from the fact that $\mathcal{S} \subset \psi_d(\mathcal{B}(0, 1))$ by the definition (4.8). \square

Proof of Theorem 4.3. This follows directly from (4.5), (4.8) and (4.22). \square

REMARK 10. In Theorem 4.3, the region $\Sigma_{\epsilon,d}$ assured to be accelerable *does not* contain some part of the real interval $[0, 1 - \epsilon]$ for any $d \geq 3$. This is consistent with Theorem 2.2.12 of [27] implying that for a linear recurrent scheme with finite memory calling the oracle T , the geometric convergence rate cannot be smaller than $1 - O(\kappa^{-1/2})$ where κ is a condition number, corresponding to ϵ^{-1} here.

4.3. Robustness of the acceleration. Note that the parameters $(\alpha_0, \dots, \alpha_{d-1})$ defined in (4.2) requires the knowledge of ϵ thus of the exact value of the spectral radius of P , which may be a restrictive assumption for practitioners. For example, in the stochastic shortest path problem analyzed in [7], we do not know the spectral radii of the substochastic matrices arising in the restricted contracting operator described in Proposition 1 of [7]. In this section we evaluate how the small perturbation of ϵ will affect the order of convergence of the acceleration scheme. This in particular allows the use of an approximate value of ϵ to compute the parameters $(\alpha_0, \dots, \alpha_{d-1})$ while still achieving an asymptotic convergence rate of order $1 - \Omega(\epsilon^{1/d})$.

For $h \geq 0$, we are looking for the smallest radius $g_\epsilon(h) \geq 0$ such that $(\phi_d^*)^{-1}(\mathcal{B}(1 - \epsilon, h)) \subset \mathcal{B}(1 - \epsilon^{1/d}, g_\epsilon(h))$, and we enforce $g_\epsilon(h) \leq \epsilon^{1/d}$ to preserve the acceleration. First we make this analysis for ψ_d (i.e. $\epsilon = 0$).

LEMMA 4.7. *For $h \geq 0$, the smallest nonnegative real number $g_0(h)$ such that*

$$\psi_d^{-1}(\mathcal{B}(1, h)) \subset \mathcal{B}(1, g_0(h))$$

is

$$g_0(h) = \frac{h^{1/d}}{(1+h)^{1/d} - h^{1/d}}, \quad \forall h \geq 0.$$

Proof. For $h = 0$, it follows from $\psi_d^{-1}(1) = \{1\}$.

Now let $h > 0$, we want to have $\psi_d(\mathcal{B}(1, g_0(h))^c) \subset \mathcal{B}(1, h)^c$, i.e.:

$$(4.29) \quad |\lambda| > g_0(h) \Rightarrow |\psi_d(1 + \lambda) - 1| > h, \quad \forall \lambda \in \mathbb{C}.$$

We have $\psi_d(1 + \lambda) = \frac{(1+\lambda)^d}{(1+\lambda)^d - \lambda^d} = 1 + \frac{\lambda^d}{(1+\lambda)^d - \lambda^d} = 1 + \frac{1}{(1+\frac{1}{\lambda})^d - 1}$, then

$$|\psi(1 + \lambda) - 1| > h \Leftrightarrow \left| \left(1 + \frac{1}{\lambda}\right)^d - 1 \right| < \frac{1}{h}, \quad \forall \lambda \in \mathbb{C}.$$

For any $\lambda \in \mathbb{C}$ we know that

$$(4.30) \quad \left| \left(1 + \frac{1}{\lambda}\right)^d - 1 \right| = \left| \sum_{k=1}^d \binom{d}{k} \frac{1}{\lambda^k} \right| \leq \sum_{k=1}^d \binom{d}{k} \frac{1}{|\lambda|^k} = \left(1 + \frac{1}{|\lambda|}\right)^d - 1.$$

Thus

$$|\lambda| > \frac{h^{1/d}}{(1+h)^{1/d} - h^{1/d}} \Leftrightarrow \left(1 + \frac{1}{|\lambda|}\right)^d - 1 < \frac{1}{h} \Rightarrow |\psi(1 + \lambda) - 1| > h, \quad \forall \lambda \in \mathbb{C}.$$

This allows to conclude because we have equality in (4.30) when $\lambda \in \mathbb{R}_+$. \square

LEMMA 4.8. For any $a \in [0, 1]$ we have

$$(\phi_d^*)^{-1}(\mathcal{B}(1 - \epsilon, a\epsilon)) \subset \mathcal{B}(1 - \epsilon^{1/d}, a^{1/d}\epsilon^{1/d}).$$

Proof. By the property (4.7) and Lemma 4.7 we deduce that for $h \geq 0$, the smallest radius $g_\epsilon(h)$ such that $(\phi_d^*)^{-1}(\mathcal{B}(1 - \epsilon, h)) \subset \mathcal{B}(1 - \epsilon^{1/d}, g_\epsilon(h))$ is given by

$$g_\epsilon(h) = \frac{(1 - \epsilon^{1/d})h^{1/d}}{(1 + h - \epsilon)^{1/d} - h^{1/d}}, \quad \forall h \geq 0.$$

Note that

$$(1 + h - \epsilon)^{1/d} - h^{1/d} \geq 1 - \epsilon^{1/d}, \quad \forall h \leq \epsilon.$$

Hence

$$g_\epsilon(h) \leq h^{1/d}, \quad \forall h \leq \epsilon.$$

We achieve the proof by taking $h = a\epsilon$. \square

The following theorem describes a d -accelerable region.

THEOREM 4.9. Let $a \in [0, 1[$, if $\text{spec } P \subset \mathcal{B}\left(0, \frac{1-\epsilon}{2^d+1}\right) \cup \mathcal{B}(1 - \epsilon, a\epsilon)$ then with the choice of α specified in (4.2) we have,

$$\text{spec } Q_{\alpha, d} \subset \mathcal{B}(0, 1 - \epsilon^{1/d}) \cup \mathcal{B}(1 - \epsilon^{1/d}, a^{1/d}\epsilon^{1/d}),$$

so that the iterates of the dA -VI algorithm (2.8) with $\beta = 0$ satisfy

$$\limsup_{k \rightarrow \infty} \|x_k - x_*\|^{1/k} \leq 1 - (1 - a^{1/d})\epsilon^{1/d}.$$

Proof. By combining Theorem 4.3, Equation (4.21) and Lemma 4.8. \square

4.4. Application to Markov Decision Processes: Accelerated Policy Iteration. As an application, we consider the standard discounted Markov decision process (MDP) with state space $[n] := \{1, \dots, n\}$, see [38, 8] for background. For each state i , denote by $\mathcal{A}(i)$ the set of actions, $P_{i,j}^a$ the transition probability from state i to state j under action $a \in \mathcal{A}(i)$, and g_i^a the reward of choosing action $a \in \mathcal{A}(i)$ in state i . Let $1 > \gamma_i > 0$, for $i \in [n]$, be state-dependent discount factors. The associated dynamic programming operator $T : \mathbb{R}^n \rightarrow \mathbb{R}^n$ is given by:

$$(4.31) \quad T_i(x) := \max_{a \in \mathcal{A}(i)} \gamma_i \sum_{j \in [n]} P_{i,j}^a x_j + g_i^a, \quad \forall i \in [n].$$

We set $\gamma := \max_{i \in [n]} \gamma_i$.

The value of the discounted problem for this MDP starting from an initial state i is given by:

$$v_i := \max_{a_0, a_1, \dots} \mathbb{E}[g_{X_0}^{a_0} + \gamma_{X_0} g_{X_1}^{a_1} + \gamma_{X_0} \gamma_{X_1} g_{X_2}^{a_2} + \dots \mid X_0 = i],$$

where the maximum is taken over admissible sequences of random actions, and X_0, X_1, \dots denotes the random sequence of states generated by the actions.

We are interested in finding the value vector $v \in \mathbb{R}^n$ of this MDP which is a solution of the fixed point problem $v = T(v)$. The fixed point exists and is unique since T is a contraction of constant γ in the sup-norm.

A classical approach to solve this problem is to use value iteration, i.e., to compute the sequence $v^k = T(v^{k-1})$, which converges to the unique fixed point. It is tempting to apply directly accelerated value iteration to the non-linear problem $v = T(v)$. This approach was proposed in [16], and it is experimentally effective on some instances. However, the convergence proof of accelerated value iteration uses inherently the affine character of the operator T , and it is not clear whether general enough convergence conditions can be given for Markov decision processes. An alternative approach, which we develop here, is to rely on *policy iteration* instead of value iteration, which will allow us to apply the idea of d th acceleration to solve MDP, but in an indirect manner, leading to convergence guarantees.

A *policy* is a map $\sigma : [n] \rightarrow \cup_{i \in [n]} \mathcal{A}(i)$ such that $\sigma(i) \in \mathcal{A}(i)$, it represents a state dependent decision rule. It determines a 0-player game, with an affine operator $T^\sigma : \mathbb{R}^n \rightarrow \mathbb{R}^n$,

$$(4.32) \quad T_i^\sigma(x) := \gamma_i \sum_{j \in [n]} P_{i,j}^{\sigma(i)} x_j + g_i^{\sigma(i)}, \quad \forall i \in [n].$$

For a vector $x \in \mathbb{R}^n$, we define the quantity $\text{top}(x) = \max_{i \in [n]} x_i$. We have $\|x\|_\infty = \max(\text{top}(x), \text{top}(-x))$. For $x, y \in \mathbb{R}^n$, we write $x \leq y$ to mean that $x_i \leq y_i$ for all $i \in [n]$. We denote by x_* the unique fixed point of the operator T and by x^σ the unique fixed point of the operator T^σ . We denote by $a^+ = \max(a, 0)$ the positive part of a real number. The following lemma presents some classical properties of the operators T and T^σ that are useful for our analysis.

LEMMA 4.10. *Let $x, y \in \mathbb{R}^n$, σ a policy, $e = (1, \dots, 1) \in \mathbb{R}^n$ the unit vector and*

$a \in \mathbb{R}^+$ a nonnegative real number, we have:

$$(4.33) \quad (\text{top}(T(x) - T(y)))^+ \leq \gamma(\text{top}(x - y))^+,$$

$$(4.34) \quad \|x - x^\sigma\|_\infty \leq \frac{1}{1-\gamma} \|x - T^\sigma(x)\|_\infty,$$

$$(4.35) \quad \|x - x_*\|_\infty \leq \frac{1}{1-\gamma} \|x - T(x)\|_\infty,$$

$$(4.36) \quad T^\sigma(x + ae) \leq T^\sigma(x) + \gamma ae,$$

$$(4.37) \quad x \leq T^\sigma(x) + ae \Rightarrow x \leq x^\sigma + \frac{a}{1-\gamma} e,$$

$$(4.38) \quad x \leq T(x) + ae \Rightarrow x \leq x_* + \frac{a}{1-\gamma} e,$$

$$(4.39) \quad x \leq y \Rightarrow T^\sigma(x) \leq T^\sigma(y).$$

Property (4.39) follows from $P_{ij}^a \geq 0$, whereas (4.36) follows from $\sum_j P_{ij}^a = 1$. Property (4.33) means that T is a contraction of rate γ in the nonsymmetric norm $(x, y) \mapsto (\text{top}(x - y))^+$. To see it we compute for $i \in [n]$, $T_i(x) - T_i(y) = \max_a \{\gamma_i \sum_{j \in [n]} P_{i,j}^a x_j + g_i^a\} - \max_a \{\gamma_i \sum_{j \in [n]} P_{i,j}^a y_j + g_i^a\} \leq (\gamma_i \sum_{j \in [n]} P_{i,j}^{a_x} x_j + g_i^{a_x}) - (\gamma_i \sum_{j \in [n]} P_{i,j}^{a_x} y_j + g_i^{a_x}) = \gamma_i \sum_{j \in [n]} P_{i,j}^{a_x} (x_j - y_j)$, where a_x is the action that maximizes the expression of $T_i(x)$. Property (4.34) (and similarly (4.35)) comes straight forward from x^σ being a fixed point of T^σ and the latter being a γ -contraction in the sup norm.

To obtain property (4.37) (and similarly (4.38)), we apply k times the operator T^σ to both sides of the initial inequality and we use the properties (4.39) and (4.36) to obtain that $x \leq (T^\sigma)^{k+1}(x) + a \sum_{i=0}^k \gamma^i e$ and finally since T^σ is a strict contraction, we know that when k goes to infinity, $(T^\sigma)^{k+1}(x)$ converges to the fixed point x^σ .

Policy iteration computes a succession of policies $\sigma^1, \sigma^2, \dots$. At each stage, it solves a 0-player fixed point problem, finding a vector v^k such that $v^k = T^{\sigma^k}(v^k)$. Then, the vector v^k is used to determine the new policy, by considering the maximizing actions in the expression of $T(v^k)$. When policy iteration is implemented in exact arithmetics, for a fixed $\gamma < 1$, the number of iterations is strongly polynomial [39]. Moreover, on ordinary instances, the number of iterations is often of a few units. Hence, the bottleneck, preventing to apply policy iteration to large scale Markov decision problems, is generally the solution of the affine problem $v^k = T^{\sigma^k}(v^k)$: algebraic methods, based on LU-factorization, are not adapted to large scale sparse instances, whereas standard iterative methods can be slow, since the contraction rate γ is typically close to 1. To address this difficulty, we present a version of policy iteration in which at each stage, v^k is computed by the d th accelerated scheme.

We consider the *Accelerated Policy Iteration of degree d (dA-PI)* presented in [Algorithm 4.1](#). Using classical estimates on approximate value iteration, see [8, 6, 34], we get the following convergence result.

PROPOSITION 4.11. *Suppose that for any policy σ , $\text{spec } P^\sigma \subset \Sigma_{\epsilon,d} \cup \{1 - \epsilon\}$, and that we choose $\alpha = (\alpha_0, \dots, \alpha_{d-2})$ as in (4.2). Each iteration k of the dA-PI algorithm terminates, and we have :*

$$(4.41) \quad \limsup_{k \rightarrow \infty} \|y_k - x_*\|_\infty \leq \frac{(1 + \gamma)\delta + \delta'}{(1 - \gamma)^2}.$$

Moreover, if $\sigma^{k+1} = \sigma^k$ for some k , then $\|y_k - x_*\|_\infty \leq \frac{\delta + \delta'}{1 - \gamma}$.

Proof. The termination of each iteration k comes from [Theorem 4.3](#). For each k , we have from the algorithm $\|y_k - T^{\sigma^k}(y_k)\|_\infty \leq \delta$, then $y_k \leq T^{\sigma^k}(y_k) + \delta e \leq T(y_k) + \delta e$. Then by (4.38) we deduce that $y_k \leq x_* + \frac{\delta}{1-\gamma} e$. Therefore $\text{top}(y_k - x_*) \leq \frac{\delta}{1-\gamma} \leq \frac{(1+\gamma)\delta + \delta'}{(1-\gamma)^2}$.

Algorithm 4.1 Accelerated Policy Iteration of degree d (dA-PI).

- 1: Fix a target accuracy δ for value determination and δ' for policy improvement.
- 2: Initialization: select a starting policy σ^0 , and set the initial values $x_{-1,0} = x_{-1,1} = \dots = x_{-1,d-2} = y_{-1,d-2} = 0$
- 3: **for** $k = 0, 1, \dots$ **do** the following:
- 4: (Accelerated value determination): Run the dA-VI (2.8) on the operator T^{σ^k} until having a residual smaller than δ : so first we initialize $x_{k,0}, x_{k,1}, \dots, x_{k,d-2}$ by the last $d-1$ values of the sequence $(x_{k-1,l})_l$ and $y_{k,d-2}$ by the last value of the sequence $(y_{k-1,l})_l$, and for $l = d-2, \dots$, we do the iterations of (2.8):

$$(4.40a) \quad x_{k,l+1} = (1 - \beta)y_{k,l} + \beta T(y_{k,l}) \quad ,$$

$$(4.40b) \quad y_{k,l+1} = (1 + \alpha_{d-2} + \dots + \alpha_0)x_{k,l+1} - \alpha_{d-2}x_{k,l} - \dots - \alpha_0x_{k,l-d+2} \quad ,$$

until $\|y_{k,l} - T^{\sigma^k}(y_{k,l})\|_\infty \leq \delta$. We denote the final $y_{k,l}$ by y_k .

- 5: (Policy improvement). We determine a policy σ^{k+1} such that $\|T(y_k) - T^{\sigma^{k+1}}(y_k)\|_\infty \leq \delta'$, and for each $i \in [n]$, we choose $\sigma^{k+1}(i) = \sigma^k(i)$ whenever possible.
 - 6: **end for**
-

We have $y_k \leq T(y_k) + \delta e \leq T^{\sigma^{k+1}}(y_k) + (\delta + \delta')e$, then by (4.37) we get $y_k \leq x^{\sigma^{k+1}} + \frac{\delta + \delta'}{1-\gamma}e$. By (4.34) and the algorithm, we have $\|y_{k+1} - x^{\sigma^{k+1}}\|_\infty \leq \|y_{k+1} - T^{\sigma^{k+1}}(y_{k+1})\|_\infty / (1-\gamma) \leq \delta / (1-\gamma)$, then $x^{\sigma^{k+1}} \leq y_{k+1} + \frac{\delta}{1-\gamma}e$. We deduce that $y_k \leq y_{k+1} + \frac{2\delta + \delta'}{1-\gamma}e$. We apply $T^{\sigma^{k+1}}$ to both sides of this inequality and use (4.39) and (4.36) to get that $T(y_k) \leq T^{\sigma^{k+1}}(y_k) + \delta'e \leq T^{\sigma^{k+1}}(y_{k+1} + \frac{2\delta + \delta'}{1-\gamma}e) + \delta'e \leq T^{\sigma^{k+1}}(y_{k+1}) + \frac{(2\delta + \delta')\gamma}{1-\gamma}e + \delta'e \leq y_{k+1} + \delta e + \frac{(2\delta + \delta')\gamma}{1-\gamma}e + \delta'e = y_{k+1} + \frac{(1+\gamma)\delta + \delta'}{1-\gamma}e$. Therefore, $x_* - y_{k+1} \leq x_* - T(y_k) + \frac{(1+\gamma)\delta + \delta'}{1-\gamma}e = T(x_*) - T(y_k) + \frac{(1+\gamma)\delta + \delta'}{1-\gamma}e$. Then $(\text{top}(x_* - y_{k+1}))^+ \leq (\text{top}(T(x_*) - T(y_k)))^+ + \frac{(1+\gamma)\delta + \delta'}{1-\gamma}$, and by using (4.33) we deduce that $(\text{top}(x_* - y_{k+1}))^+ \leq \gamma(\text{top}(x_* - y_k))^+ + \frac{(1+\gamma)\delta + \delta'}{1-\gamma}$. By iterating this inequality, we deduce that for iteration k , $(\text{top}(x_* - y_k))^+ \leq \gamma^k(\text{top}(x_* - y_0))^+ + \frac{(1+\gamma)\delta + \delta'}{1-\gamma} \sum_{i=0}^{k-1} \gamma^i$. Therefore, $\limsup_{k \rightarrow \infty} (\text{top}(x_* - y_k))^+ \leq \frac{(1+\gamma)\delta + \delta'}{(1-\gamma)^2}$, and by using $\|x_* - y_k\|_\infty = \max(\text{top}(y_k - x_*), (\text{top}(x_* - y_k))^+)$ we end the proof of (4.41).

Now, if $\sigma^{k+1} = \sigma^k$ for some k , then $\|T(y_k) - T^{\sigma^k}(y_k)\|_\infty \leq \delta'$ and we know that $\|y_k - T^{\sigma^k}(y_k)\|_\infty \leq \delta$, then $\|y_k - T(y_k)\|_\infty \leq \delta + \delta'$. Therefore by (4.35), we get $\|y_k - x_*\|_\infty \leq \frac{\delta + \delta'}{1-\gamma}$. \square

REMARK 11. Proposition 4.11 should be compared with [8, Prop. 6.2] and Remark 5 and Eqn 22 of [34], which bound the same limsup by an expression of the form $(\delta' + 2\gamma\epsilon)/(1-\gamma)^2$, where ϵ is an upper bound of $\|y_k - x^{\sigma^k}\|_\infty$. Here, ϵ is replaced by δ , which is an upper bound of the residual $\|y_k - T^{\sigma^k}(y_k)\|_\infty$.

REMARK 12. Proposition 4.11 is only an asymptotic result. In contrast, when policy iteration is implemented exactly, the value vector v^k associated to the k th policy that is selected satisfies $\|v_k - x_*\|_\infty \leq \gamma^k \|v_0 - x_*\|_\infty$, see Lemma 6.5 of [17].

REMARK 13. Since accelerated value iteration, and so, accelerated policy iteration, are implemented with a fixed precision arithmetics, one may wonder whether acceleration leads to numerical unstabilities. In the numerical experiments which follows, no such unstabilities

were observed for the relevant values $d = 2, 4$ considered here. We verified the validity of the approximate solutions that we obtained using the inequality (4.35). Indeed, the residual $\|y_k - T(y_k)\|_\infty$, where y_k is the approximate solution gotten at the final iteration of the algorithm, can be evaluated in an accurate way (with a precision close to the machine precision) using only the last value y_k . So, if this residual is small, by the inequality (4.35), we can certify that $\|y_k - x^*\|_\infty$ is also small, so that we have a valid approximate solution. In all the experiments of Section 5, the algorithms are stopped with a residual of $< 10^{-10}$, and $1 - \gamma$ is $\geq 10^{-4}$, so, it is guaranteed that the true solution is approximated with a precision $< 10^{-6}$.

5. Numerical results. In this section, we show the numerical performance of the proposed dA -VI and dA -PI with $d = 2$ and $d = 4$. The acceleration parameters in all the examples follow (4.2); the parameter $\alpha = \frac{1-\sqrt{\epsilon}}{1+\sqrt{\epsilon}}$ for accelerations of degree 2, and the parameters $\alpha_0 = \frac{(1-\epsilon^{1/4})^4}{1-\epsilon}$, $\alpha_1 = \frac{-4(1-\epsilon^{1/4})^3}{1-\epsilon}$ and $\alpha_2 = \frac{6(1-\epsilon^{1/4})^2}{1-\epsilon}$ for accelerations of degree 4.

In all the examples below, we do the policy improvement at each iteration k of the dA -PI algorithm in an exact way by taking, for each $i \in [n]$, $\sigma^{k+1}(i) \in [m]$ to be a value achieving the maximum when evaluating (4.31) at $x = y_k$, i.e. $\delta' = 0$, and we let the accuracy of the value determination to be $\delta = 10^{-10}$.

5.1. Markov decision processes with random matrices. We consider the discounted MDP model of (4.31). We take a damping parameter $\beta = 1$ in what follows.

The instances used in Figures 5.1 to 5.6 are generated in the following way. We fix two integers n and m . For each $i \in [n]$, we take $\mathcal{A}(i) = [m]$ and randomly generate a probability vector $p_i^a = (P_{i,1}^a, \dots, P_{i,n}^a)$ as follows: $P_{i,j}^a = \frac{X_{i,j}^a}{X_{i,1}^a + \dots + X_{i,n}^a}$, where the $X_{i,j}^a$ are independent Bernoulli random variables of mean $p \in (0, 1)$. The discount factors γ_i are randomly chosen in the interval $[1 - 2\epsilon, 1 - \epsilon]$, independently for each $i \in [n]$.

Let $\lambda_1, \dots, \lambda_n$ be the eigenvalues of $\sqrt{n}P$. It is shown in [9] that the counting probability measure $\frac{\delta_{\lambda_1} + \dots + \delta_{\lambda_n}}{n}$, converges weakly as $n \rightarrow \infty$ to the uniform law on the disk $\{z \in \mathbb{C} : |z| \leq \sqrt{(1-p)/p}\}$. Moreover, Theorem 1.2, *ibid.* shows that the second modulus of an eigenvalue of P is of order $1/\sqrt{n}$. This explains the shape of the spectrum shown on the figures Figures 5.1 to 5.3, and explains also, along with (4.21), why the accelerated schemes of order 4 work in the large scale example of Figure 5.6 where we take $p = 0.0025$ with $n = 10^5$.

In Figure 5.1, we consider an instance where the matrices are randomly generated as above with $n = 30$, $m = 10$ and $p = 0.2$. In subfigure 5.1(b), we display the spectrum of one matrix $P_\gamma^\sigma := (\gamma_i P_{ij}^\sigma)_{ij}$. One can notice that this spectrum presents eigenvalues that are outside the simply and multiply accelerable regions delimited respectively by Γ_ϵ and $\Gamma_{\epsilon,4}$ (see Theorem 4.3). Therefore, the accelerated policy iteration algorithms (dA -PI) cannot be applied for this instance. In accordance with that, the subfigure 5.1(a) shows that the accelerated value iteration algorithms 2A-VI and 4A-VI do not converge.

In Figure 5.2, we consider an instance with $n = 100$, $m = 10$ and $p = 0.2$. The subfigure 5.2(b) shows that the spectrum of the random matrices in this case is located in the simply accelerable region delimited by Γ_ϵ , but it is not included in the 4-accelerable region $\Gamma_{\epsilon,4}$. Therefore, we can apply the 2A-PI algorithm but not the 4A-PI in this case. The subfigure 5.2(a) shows that the simply accelerated schemes 2A-PI and 2A-VI has significantly better performances than value iteration algorithm. It shows also as expected that the acceleration of order 4 does not converge.

In Figure 5.3, we consider an instance with $n = 1500$, $m = 10$ and $p = 0.2$. The subfigure 5.3(b) shows that the spectrum of the random matrices in this case is located inside

the accelerable regions of order 2 and 4 delimited respectively by Γ_ϵ and $\Gamma_{\epsilon,4}$. Therefore, we can apply both 2A-PI and 4A-PI in this case. The subfigure 5.3(a) shows that all the accelerated schemes converge in this case and that the multi-accelerated schemes have better performances than the simply accelerated ones.

In Figure 5.4, we consider an instance with $n = 4000$, $m = 10$, $p = 0.1$. In this example we take $\epsilon = 10^{-2}$ to allow the Value Iteration algorithm to have a visible improvement.

In Figure 5.5, we consider an instance with $n = 4 \times 10^4$, $m = 10$ and the matrices used are sparse with a parameter $p = 0.005$.

We observe that the classical Policy Iteration (PI) algorithm [18, 29], using LU decomposition to solve the linear 0-player problem at each iteration, is way more faster than our iterative algorithms (dA -PI and dA -VI) in the case of small matrices like in Figures 5.1 and 5.2, but as the size of the matrices gets bigger our iterative algorithms become more competitive like in Figures 5.3 and 5.4, and even way faster than Policy Iteration like in Figure 5.5.

The Figure 5.6 represents a large scale analogue to the previous examples where the number of states is $n = 10^5$, and the matrices used are sparse with a parameter $p = 0.0025$. For this example, the classical Policy Iteration algorithm cannot be used because of memory saturation. However, the dA -PI algorithms 4.1 that we propose, with $d = 2$ and $d = 4$ here, work in this case and show significantly better performances than the classical Value Iteration algorithm. The dA -VI algorithms also show competitive performances in comparison with dA -PI algorithms. However, we expect in general that dA -PI becomes more competitive than dA -VI when the number of actions m is large, because the number of policies visited grow slowly with the number of actions (in the discounted case, a worst case almost linear bound for this number is given in [33], based on [39], the convergence being generally faster on typical instances).

In particular, for all the examples in Figures 5.2 to 5.6, we notice that both 2A-PI and 4A-PI stop only after $k \leq 5$ iterations over policies because each one of them finds a policy σ^{k+1} equal to σ^k . The same phenomenon occurs in the second application shown in the next section (see Figures 5.8 and 5.10 below).

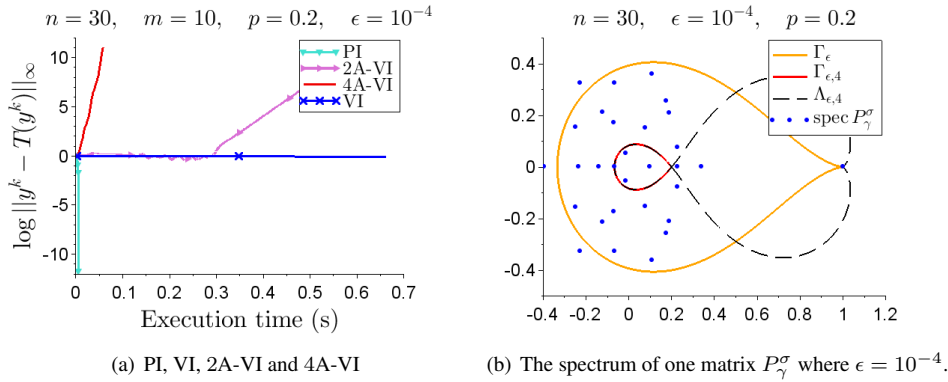


FIGURE 5.1. Markov Decision Process with random Markov matrices of size $n = 30$ and with $m = 10$ actions at each state.

5.2. Hamilton-Jacobi-Bellman PDE. We now apply the accelerated schemes to solve a Hamilton-Jacobi-Bellman (HJB) equation arising from a controlled diffusion problem with a small drift.

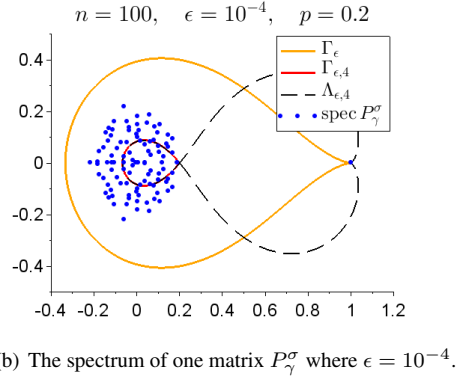
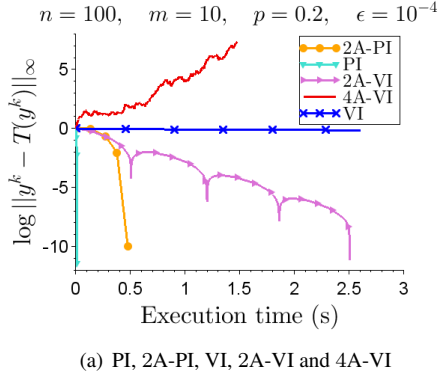


FIGURE 5.2. Markov Decision Process with random Markov matrices of size $n = 100$ and with $m = 10$ actions at each state.

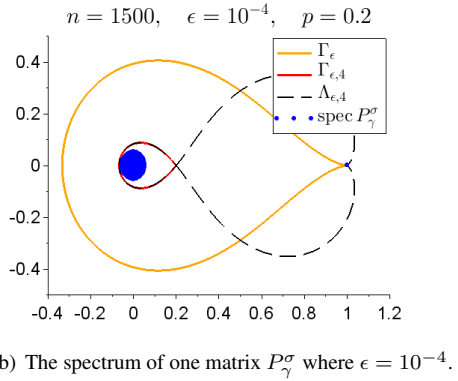
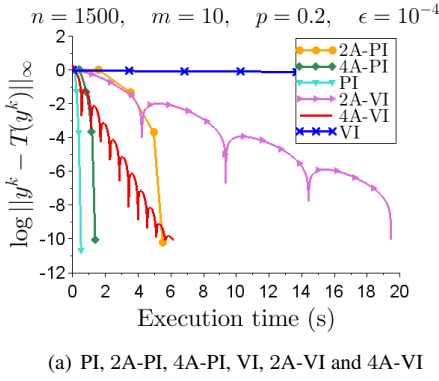


FIGURE 5.3. Markov Decision Process with random Markov matrices of size $n = 1500$ and with $m = 10$ actions at each state.

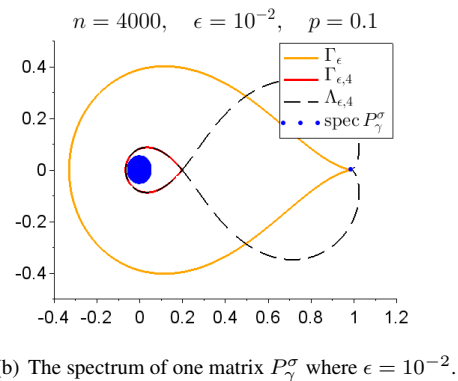
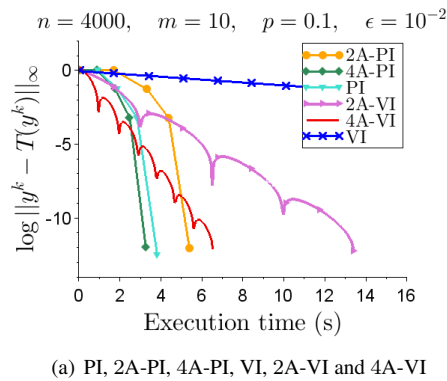


FIGURE 5.4. Markov Decision Process with random Markov matrices of size $n = 4000$ and with $m = 10$ actions at each state.

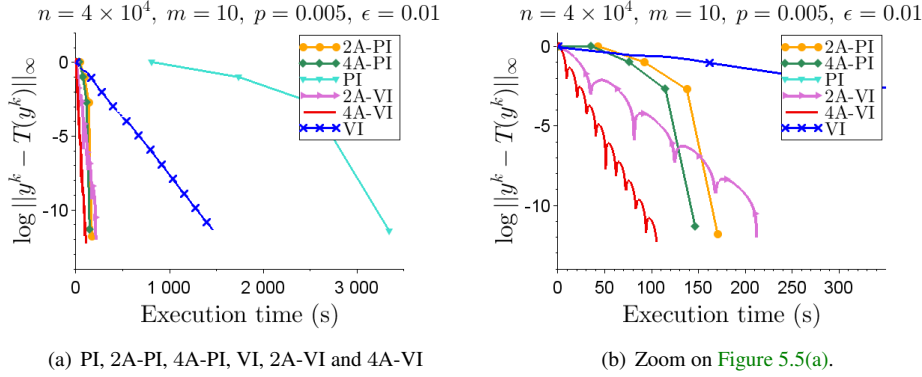


FIGURE 5.5. Markov Decision Process with random Markov matrices of size $n = 4 \times 10^4$ and with $m = 10$ actions at each state.

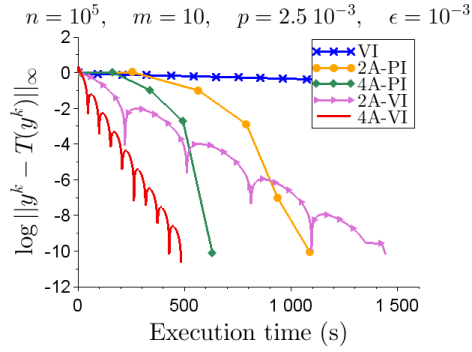


FIGURE 5.6. Markov Decision Process with random Markov matrices of size $n = 10^5$ and with $m = 10$ actions at each state.

5.2.1. Description of the problem. We consider an HJB equation in dimension $p \geq 1$, where v is a real-valued function defined on the torus $\mathbb{R}^p / \mathbb{Z}^p$, identified to $[0, 1]^p$, assuming a cyclic boundary condition:

$$(5.1) \quad \max_{a \in [m]} \left(\frac{1}{2} \sum_{i=1}^p \sigma_i^2 \frac{\partial^2 v}{\partial x_i^2}(x) + \sum_{i=1}^p g_i(a, x) \frac{\partial v}{\partial x_i}(x) - \lambda v(x) + r(a, x) \right) = 0, \quad x \in [0, 1]^p,$$

where $[m] = \{1, \dots, m\}$ is the set of actions, the scalar $\sigma_i > 0$ represents the volatility in direction i , $g_i : [m] \times [0, 1]^p \mapsto \mathbb{R}$ represents the drift in direction i that depends on the action a and the state x , $\lambda > 0$ is a dissipation parameter and $r : [m] \times [0, 1]^p \mapsto \mathbb{R}$ is the function of rewards.

The function v is given by

$$v(x) = \sup_{a(\cdot)} \mathbb{E} \left[\int_0^\infty \exp(-\lambda t) r(a(t), X_t) dt \mid X_0 = x \right],$$

with $dX_t = g(a(t), X_t)dt + \text{diag}(\sigma)dW_t$, where W_t is the standard Brownian motion on \mathbb{R}^p , $\text{diag}(\sigma)$ is the diagonal matrix with entries $(\sigma_i)_{i \in [p]}$ and the supremum is taken over progressively measurable processes $a(t)$ with respect to the filtration of the Brownian motion W_t , see [14] for background.

For $x = (x_1, \dots, x_p)$ and $i \in [p]$, we denote by $x_{\neq i}$ the $p - 1$ entries of x that are different from i . For a scalar $g \in \mathbb{R}$, we denote $g^+ = \max(g, 0)$ and $g^- = \max(-g, 0)$.

We use a uniform grid $\Omega = \{h, 2h, \dots, Nh\}^p$ to discretize the space $[0, 1]^p$, where N is a positive integer and $h = 1/N$. An upwind finite difference discretization of the HJB equation (5.1) leads to

$$(5.2) \quad \max_{a \in [m]} \left(\frac{1}{2} \sum_{i=1}^p \sigma_i^2 \frac{v(x_{\neq i}, x_i + h) + v(x_{\neq i}, x_i - h) - 2v(x)}{h^2} \right. \\ \left. + \sum_{i=1}^p g_i(a, x)^+ \frac{v(x_{\neq i}, x_i + h) - v(x)}{h} \right. \\ \left. + \sum_{i=1}^p g_i(a, x)^- \frac{v(x_{\neq i}, x_i - h) - v(x)}{h} - \lambda v(x) + r(a, x) \right) = 0, \quad x \in \Omega .$$

This equation reduces to a finite dimensional dynamic programming equation of the form $V = T(V)$, with T as in (4.31), see [23] for background. We next recall this transformation, in order to apply our method.

We consider a discrete vector $V = (V_k)_{k \in [N]^p} \in \mathbb{R}^{N^p}$ such that for each index $k = (k_1, \dots, k_p) \in [N]^p$, the k th entry of V is $V_k = v(hk)$.

The equation (5.2) can be rewritten in the following matrix form:

$$(5.3) \quad \max_{\tau \in [m]^{N^p}} (A_h^\tau V + r^\tau) = 0$$

such that for a given policy $\tau : [N]^p \rightarrow [m]$, the matrix $A_h^\tau \in \mathbb{R}^{N^p \times N^p}$ has the k th row $(A_h^\tau)_{k, \cdot}^{\tau(k)}$, $k \in [N]^p$, that represents the equation (5.2) for $x = hk \in \Omega$ and $a = \tau(k) \in [m]$, and where the vector r^τ has the k th entry $r_k^{\tau(k)} = r(\tau(k), hk)$.

We can easily see from (5.2) that the diagonal entries of each matrix A_h^τ are negative, while all the other entries are nonnegative, and this is due to the distinction of the positive and negative parts of the functions g_i that we did. We transform the problem (5.3) by introducing for each policy τ the matrix $P_h^\tau = I + ch^2 A_h^\tau$, where c is a positive scalar that allows all the matrices P_h^τ to have nonnegative entries. The following lemma shows how such a scalar can be chosen.

LEMMA 5.1. *If $c \leq c_0 := 1/(\sum_{i=1}^p \sigma_i^2 + h \max_{a \in [m], k \in [N]^p} \sum_{i=1}^p |g_i(a, hk)| + h^2 \lambda)$, then for each policy τ , all the entries of the matrix P_h^τ are nonnegative.*

Moreover, we have $P_h^\tau e = (1 - ch^2 \lambda)e$, where $e = (1, \dots, 1) \in \mathbb{R}^{N^p}$, and then $\text{spec } P_h^\tau \subset \mathcal{B}(0, 1 - \epsilon)$ with $\epsilon = ch^2 \lambda$.

Proof. By construction of P_h^τ , all its non-diagonal entries are nonnegative.

For $k \in [N]^p$, we can see from equation (5.2) that

$$(A_h^\tau)_{kk} = - \sum_{i=1}^p \sigma_i^2 / h^2 - \sum_{i=1}^p (g_i(\tau(k), hk)^+ + g_i(\tau(k), hk)^-) / h - \lambda.$$

Therefore $(P_h^\tau)_{kk} = 1 - ch^2 \lambda - c \sum_{i=1}^p \sigma_i^2 - ch \sum_{i=1}^p |g_i(\tau(k), hk)|$. Then if $c \leq c_0$, all the diagonal entries of P_h^τ are also nonnegative.

The property $P_h^\tau e = (1 - ch^2 \lambda)e$ can be easily seen when we take v equal to the constant vector e in the equation (5.2), and since all the entries of P_h^τ are nonnegative, we deduce that its spectral radius is $1 - ch^2 \lambda$ which ends the proof of the lemma. \square

REMARK 14. We notice that the parameter c used in the definition of P_h^τ plays the role of a Krasnosel'skiĭ-Mann damping (see (2.4a)). So if we divide c by 2, i.e. we take $c \leq c_0/2$, this ensures that all the eigenvalues of the matrix P_h^τ has a real part in the interval $[0, 1 - \epsilon]$.

Now, we can write the equation (5.2), as a fixed point problem that represents a 1-player game:

$$(5.4) \quad T(V) = V$$

where

$$T(V) = \max_{\tau \in [m]^n} (P_h^\tau V + r_h^\tau) .$$

with $r_h^\tau = ch^2 r^\tau$.

5.2.2. Study of the eigenvalues for uncontrolled PDE with uniform drifts. We will restrict the study of the eigenvalues of the matrices defining the problem (5.2), to the uncontrolled case where $m = 1$. We have only one matrix A_h , and $P_h = I + ch^2 A_h$. We suppose also that the drift coefficients $g_i \in \mathbb{R}$ does not depend on the state x . Under this framework we have the following lemma that gives an explicit expression of the eigenvalues of P_h .

LEMMA 5.2. *The N^p eigenvalues of the matrix P_h are given as follows for each $k \in [N]^p$:*

$$\eta(k) = 1 - c \sum_{j=1}^p \sigma_j^2 (1 - \cos(2\pi k_j h)) - c\lambda h^2 + 2ich \sum_{j=1}^p \sin(\pi k_j h) (g_j^+ e^{i\pi k_j h} - g_j^- e^{-i\pi k_j h}) .$$

Proof. For a given $k \in [N]^p$, we define the vector $V \in \mathbb{R}^{[N]^p}$ which $l \in [N]^p$ entry is given by $V_l = e^{2i\pi h \sum_{j=1}^p k_j l_j}$. From (5.2), we can verify that

$$(5.5) \quad (A_h V)_l = V_l \left(\frac{1}{2} \sum_{j=1}^p \sigma_j^2 \frac{e^{2i\pi h k_j} - 2 + e^{-2i\pi h k_j}}{h^2} + \sum_{j=1}^p \left(g_j^+ \frac{e^{2i\pi h k_j} - 1}{h} - g_j^- \frac{1 - e^{-2i\pi h k_j}}{h} \right) - \lambda \right) .$$

Then this shows that

$$\mu(k) := \sum_{j=1}^p \sigma_j^2 (\cos(2\pi k_j h) - 1)/h^2 - \lambda + 2i \sum_{j=1}^p \frac{\sin(\pi k_j h)}{h} (g_j^+ e^{i\pi k_j h} + g_j^- e^{-i\pi k_j h})$$

is an eigenvalue of the matrix A_h , and this allows to find all the N^p eigenvalues of A_h and therefore those of P_h also. \square

LEMMA 5.3. *The eigenvalues of the matrix P_h satisfy the following inequality:*

$$|\operatorname{Im}(\eta(k))| \leq \left(\sum_{j=1}^p \frac{2g_j^2}{\lambda \sigma_j^2} \right)^{\frac{1}{2}} \sqrt{\epsilon(1 - \epsilon - \operatorname{Re}(\eta(k)))}, \quad k \in [N]^p .$$

Proof. From Lemma 5.2 and using that $g_j^+ - g_j^- = g_j$, $g_j^+ + g_j^- = |g_j|$ and $\epsilon = c\lambda h^2$, we deduce that the real and imaginary parts of the eigenvalue $\eta(k)$ are:

$$\operatorname{Im}(\eta(k)) = 2ch \sum_{j=1}^p g_j \sin(\pi k_j h) \cos(\pi k_j h) ,$$

$$\operatorname{Re}(\eta(k)) = 1 - \epsilon - 2c \sum_{j=1}^p (\sigma_j^2 + h|g_j|)(\sin(\pi k_j h))^2 .$$

By using Cauchy-Schwartz inequality, we have:

$$\sum_{j=1}^p |g_j \sin(\pi k_j h)| \leq \left(\sum_{j=1}^p \frac{g_j^2}{\sigma_j^2} \right)^{\frac{1}{2}} \left(\sum_{j=1}^p \sigma_j^2 (\sin(\pi k_j h))^2 \right)^{\frac{1}{2}} .$$

and this implies the desired inequality. \square

Recall that if the spectrum of a matrix is in the region $\Sigma_\epsilon(r)$ with the choice of r shown in [Figure 3.2\(b\)](#), the 2A-VI algorithm, applied to this matrix, converges with an asymptotic rate $1 - \sqrt{\epsilon}/2$ (see [Remark 6](#)). It follows from [Lemma 5.3](#) that for a fixed value of ϵ , if the drift coefficients g_i are sufficiently small, the spectrum of the matrix P_h lies in a small neighborhood of the real segment $[0, 1 - \epsilon]$, and so it satisfies the condition for acceleration with the latter asymptotic rate. Moreover, when ϵ is small, one can show using the same lemma that the acceleration conditions are met even for drift coefficients of order 1 (this involves a long and routine verification that we skip here). We illustrate these properties in the next section.

5.2.3. Numerical results. In [Figures 5.7](#) and [5.8](#) we consider the HJB equation [\(5.1\)](#) in one dimension $p = 1$. We take the size of the discretization grid $N = 500$ with $m = 10$ actions at each state. We take the volatility $\sigma_1 = 1$ and the dissipation parameter $\lambda = 1$. We generate the drift values $g_1(a, x)$ at each state x and for each action a randomly uniformly in the interval $[0, 1]$ and we generate the rewards $r(a, x)$ randomly uniformly in $[0, 100]$. In [subfigure 5.7\(a\)](#) we display the spectrum of one matrix P_h^r . The [subfigure 5.7\(b\)](#) shows a zoom on this spectrum around the point 1, where all the difficulty occurs. It shows that the eigenvalues of P_h^r are not included in the peaked curve Γ_ϵ but are instead included in the more tolerant curve $\Gamma_\epsilon(r)$ with $r = (1 - \sqrt{\epsilon}/2)/(1 - \sqrt{\epsilon})$.

In [Figure 5.8](#), we display the performance of value iteration, accelerated policy iteration and accelerated value iteration of degree 2.

[Figures 5.9](#) and [5.10](#) display the analogue plots as [Figures 5.7](#) and [5.8](#) with an HJB equation in dimension $p = 2$, with $N = 30$, $\sigma_1 = \sigma_2 = \sqrt{2}$, $\lambda = 2$, drifts $g_1(a, x)$ in the first direction generated uniformly randomly in $[0, 1]$, drifts $g_2(a, x)$ in the second direction generated uniformly randomly in $[-1, 0]$ and rewards $r(a, x)$ generated randomly uniformly in $[0, 100]$.

We see that for these examples the accelerated algorithms 2A-VI and 2A-PI converge and are faster than the classical Value Iteration algorithm.

We mention though that on these two examples the classical Policy Iteration algorithm is way faster than 2A-PI and 2A-VI, which is expected since the size of the matrices is small, as seen in [Figures 5.1](#) to [5.6](#). However, when the size of the matrices gets bigger our iterative algorithms become faster than Policy Iteration like in the large scale example of [Figure 5.5](#).

6. Conclusion. In this paper, we solved affine fixed point problems of type $x = g + Px$, where P is a non-symmetric matrix. We showed that, if the spectrum of P is contained in an explicit region of the complex plane, a Nesterov's acceleration applied to the classical value iteration algorithm does converge with an accelerated asymptotic rate of $1 - \epsilon^{1/2}$, instead of the standard rate of $1 - \epsilon$. Moreover, we introduced a new accelerated algorithm, of order $d \geq 2$, and showed that, under a more demanding condition on the spectrum of P , this algorithm converges with a multiply accelerated asymptotic rate of $1 - \epsilon^{1/d}$. Using these accelerated schemes, we developed an accelerated policy iteration algorithm that solves non-linear fixed point problems arising from Markov decision processes. We illustrated the

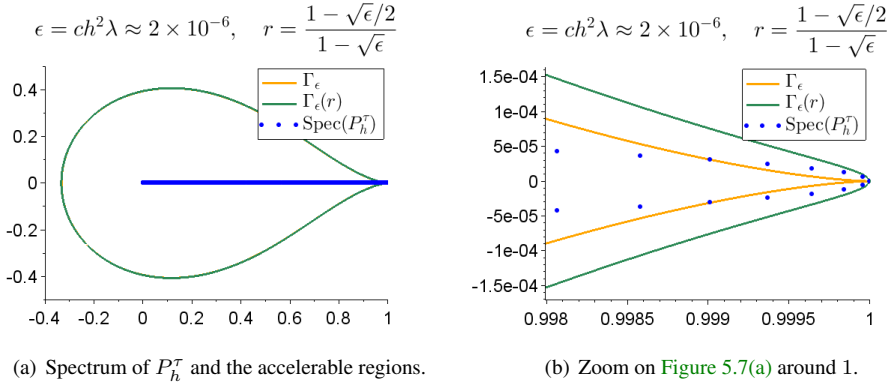


FIGURE 5.7. Spectrum of the matrix P_h^T and acceleration region, for the HJB PDE in dimension one

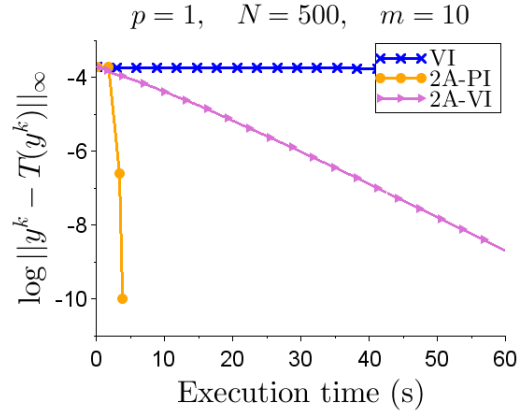


FIGURE 5.8. Solving HJB equation in one dimension with $N = 500$, $\lambda = 1$, $\sigma_1 = 1$, $g_1 \sim \mathcal{U}([0, 1])$, $c = c_0/2 \approx 0.5$, $\epsilon = ch^2\lambda \approx 2 \times 10^{-6}$ and $r \sim \mathcal{U}([0, 100])$.

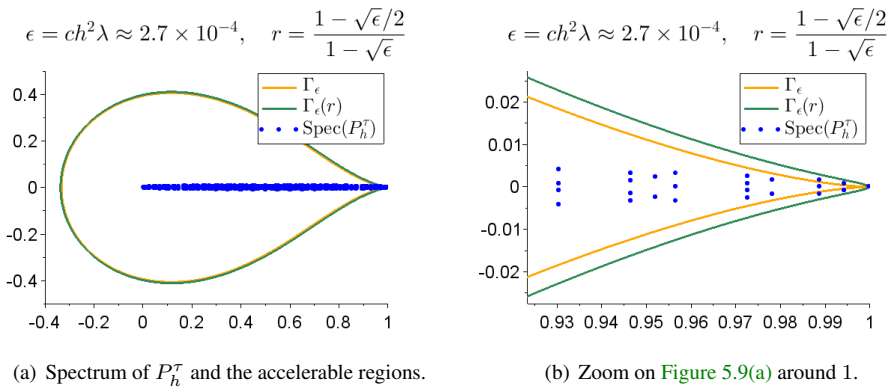


FIGURE 5.9. Spectrum of the matrix P_h^T and acceleration region, for the HJB PDE in dimension two

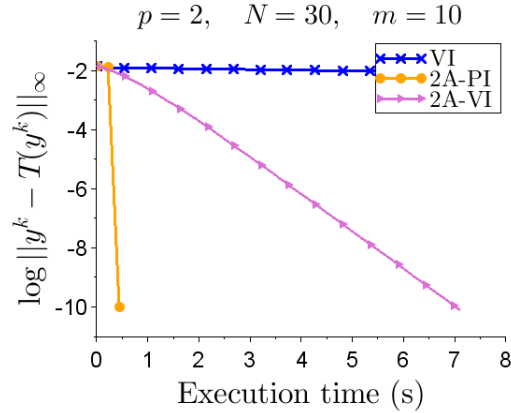


FIGURE 5.10. Solving HJB equation in two dimensions with $N = 30$, $\lambda = 2$, $\sigma_1 = \sigma_2 = \sqrt{2}$, $g_1 \sim \mathcal{U}([0, 1])$, $g_2 \sim \mathcal{U}([-1, 0])$, $c = c_0/2 \approx 0.12$, $\epsilon = ch^2\lambda \approx 2.7 \times 10^{-4}$ and $r \sim \mathcal{U}([0, 100])$.

performance of the accelerated schemes on two frameworks, one using random matrices and the second solving an Hamilton-Jacobi-Bellman equation. As an open problem, it remains to generalize the convergence analysis of the accelerated value iteration algorithm, of degree $d \geq 2$, to the case of non-linear fixed point problems, and in particular to Markov decision processes.

REFERENCES

- [1] D. ANDERSON, *Iterative procedures for nonlinear integral equations*, Journal of the ACM, 12 (1965), pp. 547–560.
- [2] H. ATTOUCH, *Fast inertial proximal ADMM algorithms for convex structured optimization with linear constraint*, Minimax Theory and its Application, 6 (2021), pp. 1–24. hal-02501604.
- [3] H. ATTOUCH AND J. PEYPOUQUET, *Convergence of inertial dynamics and proximal algorithms governed by maximally monotone operators*, Mathematical Programming, 174 (2019), pp. 391–432.
- [4] J. B. BAILLON AND R. E. BRUCK, *The rate of asymptotic regularity is $O(1/\sqrt{n})$* , Lecture Notes in Pure and Applied Mathematics, (1996), pp. 51–81.
- [5] R. BELLMAN, *Dynamic Programming*, Princeton University Press, Princeton, NJ, 1957.
- [6] D. P. BERTSEKAS, *Approximate policy iteration: A survey and some new methods*, Journal of Control Theory and Applications, 9 (2011), pp. 310–335.
- [7] D. P. BERTSEKAS AND J. N. TSITSIKLIS, *An analysis of stochastic shortest path problems*, Mathematics of Operations Research, 16 (1991), pp. 580–595.
- [8] D. P. BERTSEKAS AND J. N. TSITSIKLIS, *Neuro-Dynamic Programming*, Athena Scientific, 1996.
- [9] C. BORDENAVE, P. CAPUTO, AND D. CHAFAI, *Circular law theorem for random Markov matrices*, Probability Theory and Related Fields, 152 (2008).
- [10] C. CHEN, S. MA, AND J. YANG, *A general inertial proximal point algorithm for mixed variational inequality problem*, SIAM Journal on Optimization, 25 (2015), pp. 2120–2142.
- [11] Y. DRORI AND M. TEBoulLE, *Performance of first-order methods for smooth convex minimization: a novel approach*, Mathematical Programming, 145 (2014), pp. 451–482.
- [12] J. ECKSTEIN AND D. P. BERTSEKAS, *On the Douglas-Rachford splitting method and the proximal point algorithm for maximal monotone operators*, Mathematical Programming, 55 (1992), pp. 293–318.
- [13] N. FLAMMARION AND F. BACH, *From averaging to acceleration, there is only a step-size*, in Proceedings of The 28th Conference on Learning Theory, P. Grünwald, E. Hazan, and S. Kale, eds., vol. 40 of Proceedings of Machine Learning Research, 03–06 Jul 2015, pp. 658–695.
- [14] W. H. FLEMING AND H. M. SONER, *Controlled Markov processes and viscosity solutions*, vol. 25, Springer Science & Business Media, 2006.
- [15] E. GHADIMI, H. R. FEYZMAHDAVIAN, AND M. JOHANSSON, *Global convergence of the heavy-ball method for convex optimization*, in 2015 European Control Conference (ECC), 2015, pp. 310–315.
- [16] V. GOYAL AND J. GRAND-CLEMENT, *A first-order approach to accelerated value iteration*, 2019.

arXiv:1905.09963.

- [17] T. D. HANSEN, P. B. MILTERSEN, AND U. ZWICK, *Strategy iteration is strongly polynomial for 2-player turn-based stochastic games with a constant discount factor*, Journal of the ACM, 60 (2013), pp. 1–16.
- [18] R. A. HOWARD, *Dynamic programming and Markov processes*, John Wiley, 1960.
- [19] F. IUTZELER AND J. M. HENDRICKX, *A generic online acceleration scheme for optimization algorithms via relaxation and inertia*, Optimization Methods and Software, 34 (2019), pp. 383–405.
- [20] A. IZMAILOV AND M. SOLODOV, *Newton-Type Methods for Optimization and Variational Problems*, Springer, 03 2014.
- [21] D. KIM, *Accelerated proximal point method for maximally monotone operators*, 2019.
- [22] M. A. KRASNOSEL'SKIĬ, *Two remarks on the method of successive approximations*, Uspekhi Matematicheskikh Nauk, 10 (1955), pp. 123–127.
- [23] H. J. KUSHNER AND P. G. DUPUIS, *Numerical methods for stochastic control problems in continuous time*, vol. 24, Springer Science & Business Media, 2001.
- [24] F. LIEDER, *On the convergence rate of the Halpern-iteration*, Optimization Letters, 15 (2021), pp. 405–418.
- [25] W. R. MANN, *Mean value methods in iteration*, Proceedings of the American Mathematical Society, 4 (1953), pp. 506–510.
- [26] Y. NESTEROV, *A method of solving a convex programming problem with convergence rate $o(1/k^2)$* , Soviet Mathematics Doklady, 27 (1983), pp. 372–376.
- [27] Y. NESTEROV, *Introductory Lectures on Convex Optimization: A Basic Course (Applied Optimization)*, Kluwer Academic Publishers, 2004.
- [28] B. POLYAK, *Some methods of speeding up the convergence of iteration methods*, USSR Computational Mathematics and Mathematical Physics, 4 (1964), pp. 1 – 17.
- [29] M. L. PUTERMAN, *Markov decision processes: discrete stochastic dynamic programming*, John Wiley & Sons, 2014.
- [30] H. REN FANG AND Y. SAAD, *Two classes of multiseccant methods for nonlinear acceleration*, Numer. Linear Algebra Appl., 16 (2009), pp. 197–221.
- [31] R. T. ROCKAFELLAR, *Augmented Lagrangians and applications of the proximal point algorithm in convex programming*, Mathematics of operations research, 1 (1976), pp. 97–116.
- [32] R. T. ROCKAFELLAR, *Monotone operators and the proximal point algorithm*, SIAM Journal on Control and Optimization, 14 (1976), pp. 877–898.
- [33] B. SCHERRER, *Improved and generalized upper bounds on the complexity of policy iteration*, in Advances in Neural Information Processing Systems, 2013, pp. 386–394.
- [34] B. SCHERRER, M. GHAVAMZADEH, V. GABILLON, B. LESNER, AND M. GEIST, *Approximate modified policy iteration and its application to the game of tetris.*, J. Mach. Learn. Res., 16 (2015), pp. 1629–1676.
- [35] D. SCIEUR, F. BACH, AND A. D'ASPREMONT, *Nonlinear acceleration of stochastic algorithms*, in Advances in Neural Information Processing Systems, I. Guyon, U. V. Luxburg, S. Bengio, H. Wallach, R. Fergus, S. Vishwanathan, and R. Garnett, eds., vol. 30, Curran Associates, Inc., 2017.
- [36] A. THEMELIS AND P. PATRINOS, *Supermann: A superlinearly convergent algorithm for finding fixed points of nonexpansive operators*, IEEE Transactions on Automatic Control, 64 (2019), pp. 4875–4890.
- [37] H. F. WALKER AND P. NI, *Anderson acceleration for fixed-point iterations*, SIAM Journal on Numerical Analysis, 49 (2011), pp. 1715–1735.
- [38] P. WHITTLE, *Optimization over time. Vol. II*, Wiley Series in Probability and Mathematical Statistics: Applied Probability and Statistics, John Wiley & Sons Ltd., Chichester, 1983.
- [39] Y. YE, *The simplex and policy-iteration methods are strongly polynomial for the Markov decision problem with a fixed discount rate*, Mathematics of Operations Research, 36 (2011), pp. 593–603.
- [40] J. ZHANG, B. O'DONOGHUE, AND S. BOYD, *Globally convergent type-I Anderson acceleration for non-smooth fixed-point iterations*, SIAM Journal on Optimization, 30 (2020), pp. 3170–3197.